

**FILM COOLING ON A FLAT PLATE: INVESTIGATING DENSITY  
AND UPSTREAM STEP EFFECTS USING IR AND PSP**

A Thesis

by

JOSHUA P. F. GRIZZLE

Submitted to the Office of Graduate Studies of  
Texas A&M University  
in partial fulfillment of the requirements for the degree of

MASTER OF SCIENCE

May 2008

Major Subject: Mechanical Engineering

**FILM COOLING ON A FLAT PLATE: INVESTIGATING DENSITY  
AND UPSTREAM STEP EFFECTS USING IR AND PSP**

A Thesis

by

JOSHUA P. F. GRIZZLE

Submitted to the Office of Graduate Studies of  
Texas A&M University  
in partial fulfillment of the requirements for the degree of  
MASTER OF SCIENCE

Approved by:

Chair of Committee,  
Committee Members,  
Head of Department,

Je-Chin Han  
Harry Hogan  
Eric Bickel  
Dennis O'Neal

May 2008

Major Subject: Mechanical Engineering

## ABSTRACT

Film Cooling on a Flat Plate: Investigating Density  
and Upstream Step Effects Using IR and PSP. (May 2008)

Joshua P. F. Grizzle, B.S., Texas A&M University

Chair of Advisory Committee: Dr. Je-Chin Han

This study is an investigation of two specific effects on turbine blade film cooling. The effect of coolant to mainstream density ratio and upstream steps was studied. The studies were conducted on two flat plates with 4mm cylindrical film cooling holes, one with simple angle and the other with compound angle, in a low-speed suction type wind tunnel.

Density effect was studied at ratios of 0.93 and 1.47 by using air and CO<sub>2</sub> as coolant. An IR camera was used to record the temperature on the plate and T-type thermocouples were used to record the coolant and mainstream temperatures. During the study the nature of the conduction effect from the heated coolant was studied and found to be most prevalent along the plate surface not through the plate from the plenum. A methodology was presented by which conduction error free results were obtained. The results showed an increased effectiveness at higher density ratios, particularly near the holes and for the simple angle plate.

Upstream step effect was studied using pressure sensitive paint and a coupled strobe light and camera. Steps of 0.5, 1 and 1.5mm were placed at the upstream edge of the holes. The steps were found to increase effectiveness significantly more than previous studies have shown when placing the step slightly upstream of the holes.

## **ACKNOWLEDGEMENTS**

I would like to thank Dr. Han for his guidance and support in my research. I would like to thank Dr. Hogan and Dr. Bickel for their mentorship and for serving on my committee. I would like to thank both Sarah Blake and Akhilesh Rallabandi for teaching and working with me in the lab. Finally, I would like to thank my parents for teaching me the value of finishing.

## NOMENCLATURE

$C_{\text{mix}}$	oxygen concentration of mainstream-coolant mixture mix
$C_{\infty}$	oxygen concentration of mainstream
$I$	emission intensity of PSP
$I_{\text{air}}$	emission intensity of PSP recorded with air as the coolant
$I_{\text{N}_2}$	emission intensity of PSP recorded with nitrogen as the coolant
$I_{\text{ref}}$	emission intensity of PSP at reference (atmospheric) pressure
$M_s$	slot injection blowing ratio, ratio of coolant momentum to mainstream momentum
$m_s$	slot injection mass flow ratio (percentage of the mainstream flow)
$(P_{\text{O}_2})_{\text{N}_2}$	partial pressure of oxygen measured with nitrogen as the coolant
$(P_{\text{O}_2})_{\text{air}}$	partial pressure of oxygen measured with air as the coolant
$\eta_{\text{film}}$	cooling effectiveness
$D$	film cooling hole diameter
$T_{\text{aw}}$	adiabatic wall temperature measured by IR camera
$T_{\infty}$	mainstream temperature measured by thermocouples
$T_c$	coolant temperature measured by thermocouples

## TABLE OF CONTENTS

	Page
ABSTRACT .....	iii
ACKNOWLEDGEMENTS.....	iv
NOMENCLATURE .....	v
LIST OF FIGURES .....	vii
LIST OF TABLES.....	ix
INTRODUCTION .....	1
Flat Plate Cooling .....	1
Density Ratio .....	2
Step Effects .....	3
Current Study.....	4
EXPERIMENTAL SETUP AND PROCEDURE.....	5
Instrumentation .....	5
Measurement Techniques .....	8
Procedure .....	14
RESULTS.....	16
Conduction Effect.....	16
Density Effect .....	18
Upstream Step Effect.....	23
CONCLUSIONS .....	34
REFERENCES .....	36
APPENDIX A.....	40
APPENDIX B.....	44
VITA.....	50

## LIST OF FIGURES

	Page
Figure 1: Turbine blade cooling technology.....	6
Figure 2: Test apparatus 3D.....	6
Figure 3: Overhead schematic of test apparatus with PSP recording device .....	7
Figure 4: Simple and compound angle cylindrical hole plates.....	8
Figure 5: IR measurement technique.....	9
Figure 6: IR calibration curve.....	10
Figure 7: How PSP works .....	11
Figure 8: Experimental setup for PSP data acquisition .....	12
Figure 9: PSP calibration apparatus.....	13
Figure 10: PSP calibration curve .....	13
Figure 11: Conduction effect over 5 minutes .....	17
Figure 12: Conduction effect on spanwise averages over time .....	17
Figure 13: Comparison of current study to previous studies.....	18
Figure 14: Contour plots of simple angle hole density effect at various blowing ratios .....	20
Figure 15: Contour plots of compound angle hole density effect at various blowing ratios .....	21
Figure 16: Spanwise average of effectiveness of simple angle holes at $M=0.6$ .....	22
Figure 17: Spanwise average of effectiveness of compound angle holes at $M=0.6$ .....	23
Figure 18: PSP film cooling effectiveness for cylindrical simple angle holes with no step.....	24
Figure 19: PSP film cooling effectiveness for cylindrical simple angle holes with 0.5 mm step.....	25
Figure 20: PSP film cooling effectiveness for cylindrical simple angle holes with 1 mm step.....	26
Figure 21: PSP film cooling effectiveness for cylindrical simple angle holes with 1.5 mm step.....	27
Figure 22: Spanwise effectiveness for various upstream steps on simple angle plate at $M = 0.6$ .....	28
Figure 23: PSP film cooling effectiveness for cylindrical compound angle holes with no step.....	29
Figure 24: PSP film cooling effectiveness for cylindrical compound angle holes with 0.5 mm step .....	30

	Page
Figure 25: PSP film cooling effectiveness for cylindrical compound angle holes with 1.0 mm step .....	31
Figure 26: PSP film cooling effectiveness for cylindrical compound angle holes with 1.5 mm step .....	32
Figure 27: Spanwise effectiveness for various upstream steps on compound angle plate at $M = 0.6$ .....	33
Figure 28: PSP spanwise average of effectiveness of simple angle holes at $M=0.3$ .....	40
Figure 29: PSP spanwise average of effectiveness of simple angle holes at $M=1.0$ .....	41
Figure 30: PSP spanwise average of effectiveness of simple angle holes at $M=1.5$ .....	41
Figure 31: PSP spanwise average of effectiveness of compound angle holes at $M=0.3$ .....	42
Figure 32: PSP spanwise average of effectiveness of compound angle holes at $M=1.0$ .....	42
Figure 33: PSP spanwise average of effectiveness of compound angle holes at $M=1.5$ .....	43
Figure 34: Spanwise effectiveness for various upstream steps on simple angle plate at $M = 0.3$ .....	44
Figure 35: Spanwise effectiveness for various upstream steps on simple angle plate at $M = 1.0$ .....	45
Figure 36: Spanwise effectiveness for various upstream steps on simple angle plate at $M = 1.5$ .....	46
Figure 37: Spanwise effectiveness for various upstream steps on compound angle plate at $M = 0.3$ .....	47
Figure 38: Spanwise effectiveness for various upstream steps on compound angle plate at $M = 1.0$ .....	48
Figure 39: Spanwise effectiveness for various upstream steps on compound angle plate at $M = 1.5$ .....	49



**LIST OF TABLES**

	Page
Table 1: Test conditions for density ratio effect.....	14
Table 2: Test conditions for step effect .....	15

## INTRODUCTION

Gas turbines are used in many aviation and power generation applications. The efficiency of gas turbines can be increased by raising the inlet temperature. The operating temperature is limited however, by the material properties of the turbine components. At sufficiently high operating temperatures the structural materials of the turbine begin to degrade. Modern turbines are able to operate at temperatures far exceeding these limits by using internal and external cooling methods to insure that the blades and other vulnerable areas remain well below the main stream temperature. Internal cooling methods include impingement, rib-turbulated passages, and pin-fin cooling. External cooling in turbines is conducted using film cooling methods. Film cooling involves the flow of coolant into the main stream at the blade surface with the purpose of providing a thin insulating boundary layer.

Film cooling technology has been one of the major advances in gas turbine design over the last 30 years. Injection of coolant into the mainstream through holes along structural surfaces in the turbine can dramatically reduce the temperature of those surfaces. Film cooling is one of the major reasons that today's high temperature, high efficiency turbines are possible and has therefore been a major focus of study during the last two decades [1].

### **Flat Plate Cooling**

Film cooling research over the last 30 years has focused on topics including freestream turbulence, surface curvature, coolant density and hole shape, all of which have a significant impact on the film cooling effectiveness [2]. Bogard et al. [3] divides the factors affecting film cooling performance into three main categories: coolant/mainstream conditions, hole geometry and airfoil geometry. The coolant density

---

This thesis follows the style of AMSE Journal of Heat Transfer.

ratio, mass flux ratio and momentum ratio affect film cooling performance as do mainstream turbulence, mach number and rotation. Hole geometry factors include hole shape, size, angle of injection, and spacing on the surface; Goldstein et al. [4] were one of the first to examine the effects of hole shape. Goldstein et al. [4, 5] and Jubran et al. [6] showed the optimum coolant to mainstream momentum ratio to be approximately  $M = 0.5$ . Additionally, hole location on the airfoil and surface curvature and roughness affect the cooling performance.

### **Density Ratio**

Understanding the effect of coolant-to-mainstream density ratio is important because of the dramatic temperature difference between coolant and mainstream flows resulting in significant differences in density. The main challenge to existing research on the effect coolant-to-mainstream density ratio has on film cooling performance is the error due to conduction. In order to achieve various density ratios, researchers have used  $\text{CO}_2$  as the coolant flowing into an air mainstream producing a density ratio of approximately 1.5. Wright et al. [7] compared the film cooling effectiveness measurement methods of Pressure Sensitive Paint (PSP), Temperature Sensitive Paint (TSP) and Infrared (IR), concluding that PSP was the most accurate method because it was not subject to conductivity errors. Unfortunately PSP is not effective in measuring  $\text{CO}_2$  which leaves only thermography methods with which to study the impact of density ratio on film cooling effectiveness.

Bell et al. [8] and Sinha et al. [9] studied density ratios 0.9 to 1.4 and avoided the conduction error by using individual thermocouples to record several discrete temperatures downstream of film cooling holes. This method however gives a very low resolution results that do not provide the full understanding of downstream effectiveness provided by thermography methods. Jessen et al [10] and Pietrzyk et al [11] have studied the density ratio effect on flat plate film cooling using Particle-Image Velocimetry (PIV)

and Laser Doppler Velocimetry (LDV) respectively, and both present precise and reasonably error free results of the flow field, not the film cooling effectiveness.

IR, TSP and Liquid Crystal Thermography require the coolant be heated or cooled from the mainstream temperature; this results in conduction along the plate which is hard to isolate from the effect of the coolant flow. Schmidt et al. [12] used the IR method to study density effect but made no mention of the conduction effect which almost certainly affected his results. Cutbirth et al. [13] has attempted to quantify the conduction effect and isolate it from the film cooling effect by recording the conduction at steady state flow through the coolant plenum but with no flow through the holes. This method assumes that the error is a result of conduction through the plate from the heated or chilled air in the plenum. The majority of the conduction though is in fact along the surface of the flat plate radiating out from the path directly downstream of the holes. Despite conduction errors these two papers presented the film cooling effectiveness as increasing with higher coolant to mainstream density ratio.

### **Step Effects**

The effect of different types of turbulence promoters upstream of the film cooling holes has also been a focus of recent film cooling research. Waye et al [14], Lu et al [15], Bunker et al [16], and Harrison et al [17] have all performed experimental investigations of the film cooling effectiveness of holes imbedded in a slot or trench. Harrison et al [18] presents a computational analysis of trench film cooling effectiveness as well. These studies concluded that the film cooling effectiveness around the holes is significantly improved when the holes are set in a trench “due to a lateral spreading of the coolant and reduced coolant jet separation” [14]. The effect of a simple step upstream of the holes though is not well defined but has potential to greatly increase effectiveness in the same way by creating a vortex at the point where the coolant enters the mainstream.

Barigozzi et al [19] studied the effect of an upstream ramp of height  $0.5D$  placed  $0.5D$  upstream of holes on a flat plate, using both a cylindrical and conical hole configuration. The study found that the ramp only increased effectiveness at very low blowing ratios but at other blowing ratios the effect was insignificant. In Barigozzi et al [20] the ramp was shown to have significant aerodynamic losses which could be a detriment to its helpfulness when implemented on a turbine blade.

### **Current Study**

The objective of this study is better define, both the effect of coolant-to-mainstream density ratio, and various upstream step geometries have on film cooling effectiveness. The study of density ratio will be focused on eliminating conduction error from the results so that more accurate depictions of the film cooling effectiveness can be developed. The study of upstream step effect will be focused on determining what effect a simple upstream step has when placed at the upstream edge of the film cooling holes. These two studies focus on areas of current research where there is a lack of full understanding, where this study could prove to advance the field.

## EXPERIMENTAL SETUP AND PROCEDURE

### Instrumentation

Study of density ratio effect and upstream step effect will be carried out independently but on the same test apparatus. In order to contextualize this procedure in the larger picture of turbine blade cooling, Figure 1 shows the configuration of film cooling holes on an actual turbine blade surface. The flat plate used in this procedure simulates a turbine blade surface with film cooling holes, and the plenum simulates the internal passage through which coolant would be routed to the holes.

The 9.0 in x 3.0 in x 0.6 in flat plate is placed in a low-speed suction type wind tunnel, which will simulate the turbine mainstream flow. The details of this particular wind tunnel can be found in Young et al [21]. The tunnel has a 4:1 contraction ratio nozzle with a straw flow straightener box at the inlet, cross-section 60.96 cm x 30.48 cm. The test channel cross section is 30.48 cm x 15.24 cm. The wind tunnel is driven by a 5.6 kW axial blower that creates suction enough to reach a maximum velocity of 34 m/s.

Attached to the underside of the plate is a plenum as shown in Figure 2. Figure 3 shows the coolant flow schematic through which air, N<sub>2</sub> or CO<sub>2</sub> can be supplied to the plenum at room temperature or heated by the 5 kW pipe heater up to temperatures of 60°F.

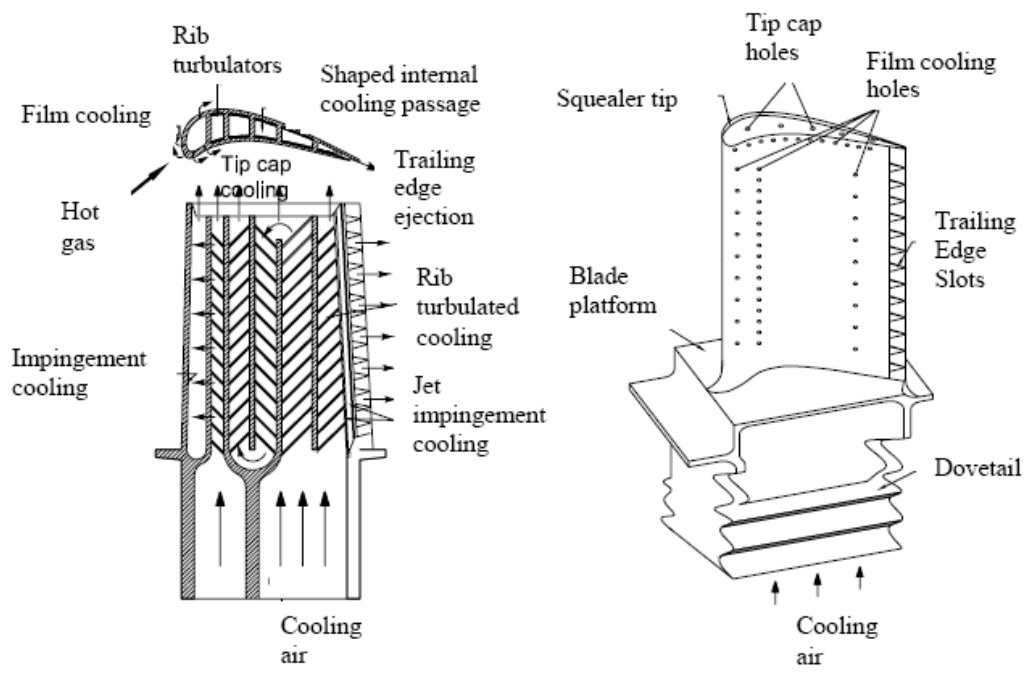


Figure 1: Turbine blade cooling technology

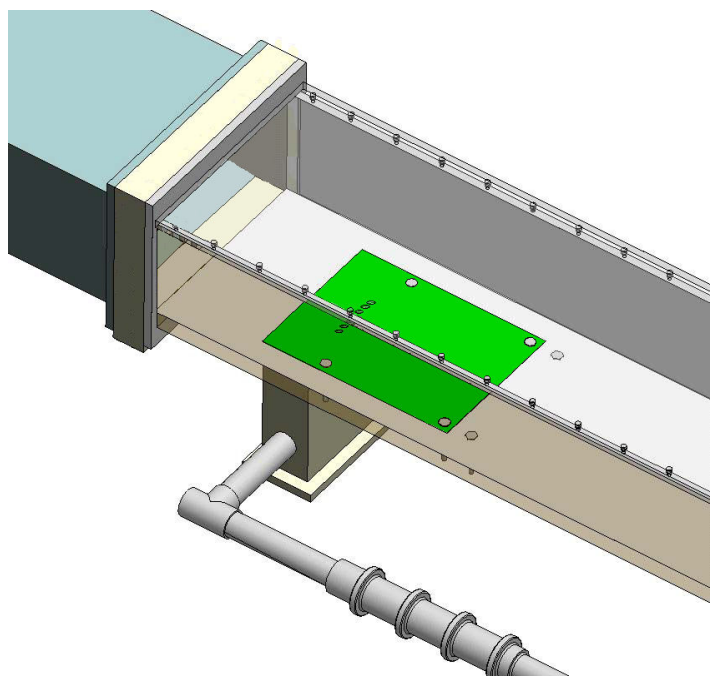
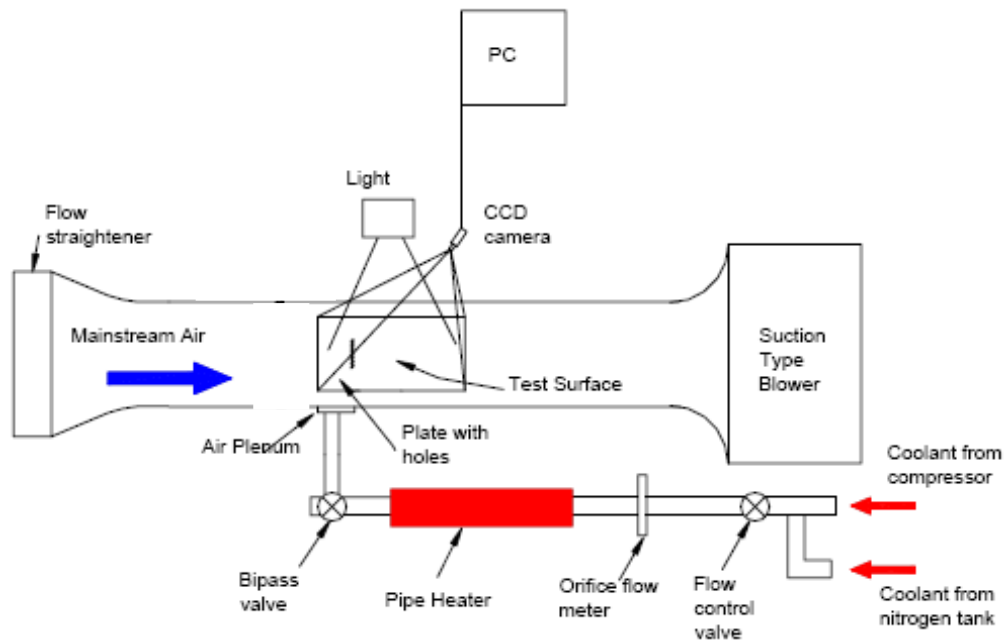


Figure 2: Test apparatus 3D



**Figure 3: Overhead schematic of test apparatus with PSP recording device**

Much of the film cooling research over the last decade has focused on hole geometry. In order to develop a comprehensive understanding of the density and step effects studied in this report multiple flat plates, each with different hole geometry, will be tested. The density ratio study will be carried out using the two plates shown in Figure 4, each with seven cylindrical holes. The holes on the first plate have a simple  $30^\circ$  angle to horizontal. The second plate has compound angle holes, both  $30^\circ$  to horizontal and  $45^\circ$  to the mainstream flow direction. Because the density ratio is being studied using IR thermography, which is susceptible to conduction error, the plates were made of Last-A-Foam with a very low coefficient of conductivity at  $0.03 \text{ W/m}^2\text{K}$ . The upstream step effect will be tested on the same two plates.



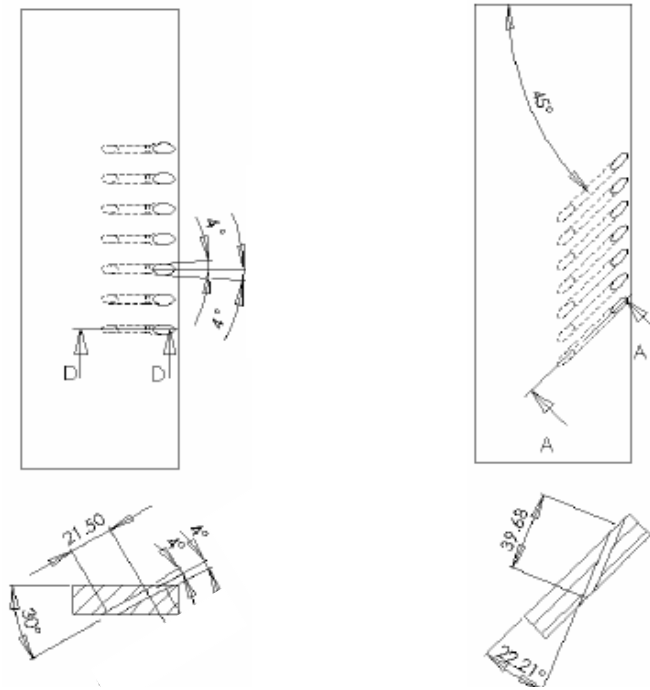


**Figure 4: Simple and compound angle cylindrical hole plates**

### **Measurement Techniques**

Measurement of the cooling effectiveness will be performed using both infrared and pressure sensitive paint techniques. IR will primarily be used to study the density effect as shown in Figure 5, which will involve injecting heated and cooled air and  $\text{CO}_2$  through the holes, with PSP as a reference point to put the IR in context. The upstream step will be studied using PSP to avoid conduction errors involved in the IR procedure.

IR thermography measures the temperature of a black surface based on an emissivity calibration. Calibration is performed by recording the temperatures of a painted copper block, with both the IR camera and imbedded thermocouples, as it is heated and then allowed to cool. After painting the surface with black paint and positioning the IR camera above it as shown in Figure 5, temperature profiles of the plate surface can be recorded. Based on the results of this calibration and the resulting correlation shown in Figure 6, the emissivity coefficient of the plate surface can be adjusted in the IR data

recorder to yield accurate, high resolution temperature data. During the experiment, there are 3 T-type thermocouples in the mainstream and 4 in the plenum recording the average temperature of the fluid in each. Using the mainstream, coolant and plate surface temperatures, film cooling effectiveness is defined by Equation 1:

$$\eta = \frac{T_{aw} - T_{\infty}}{T_c - T_{\infty}} \quad (1)$$

This technique is explained in more depth in Han [22] and used by Wright et al [7] and Dittmar et al [23].

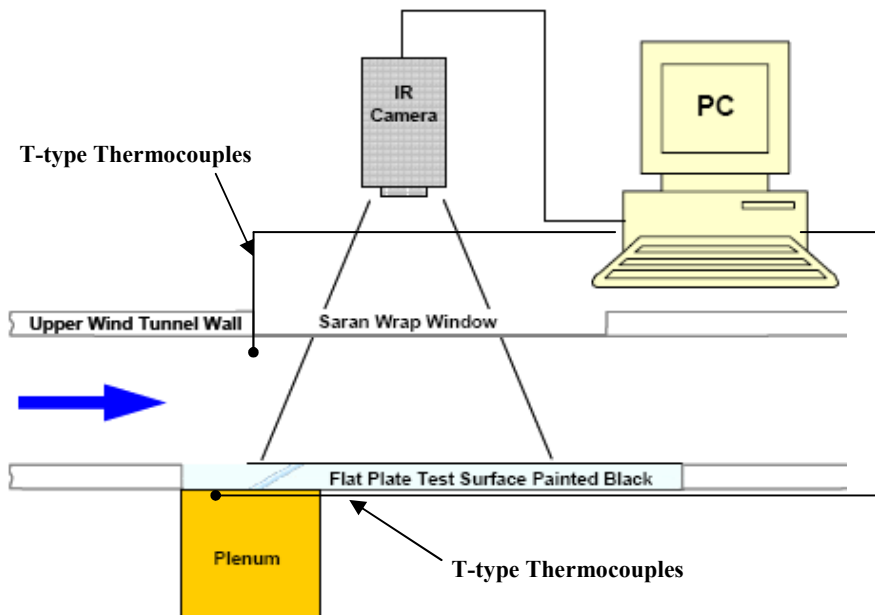


Figure 5: IR measurement technique

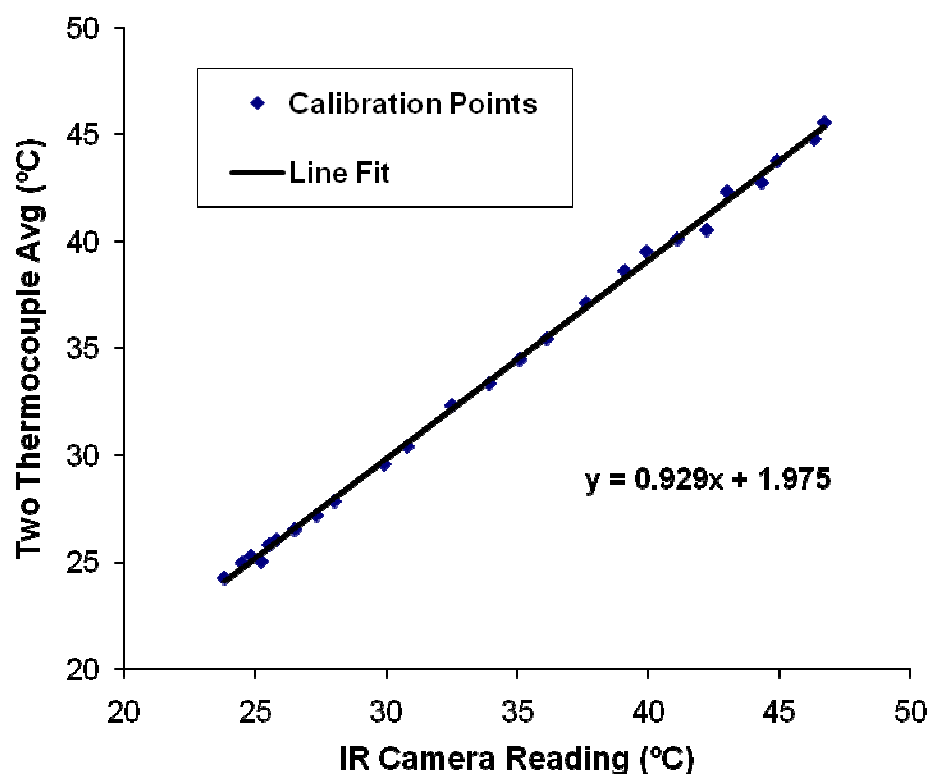


Figure 6: IR calibration curve

The study of upstream step effects will be conducted using Pressure Sensitive Paint (PSP), which contains oxygen-quench photoluminescence. When excited by a light source, these particles illuminate at varying intensity depending on the partial pressure of oxygen. To measure the film-cooling effectiveness pure nitrogen is used as the coolant, while air (21% oxygen) flows through the mainstream. When properly calibrated, the PSP intensity values yielded by the camera images represent the concentration of oxygen on the plate surface. This method is discussed in Han [22] and Zhang [24], and is also used by Crafton et al [25] and Liu et al [26].

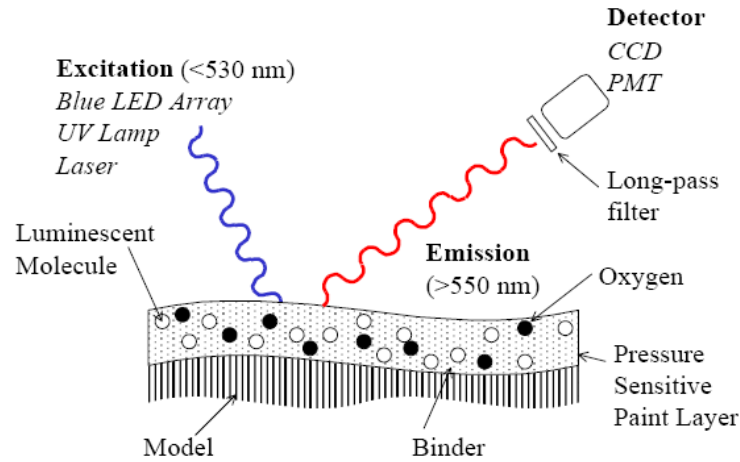


Figure 7: How PSP works

The oxygen concentration measurements  $C$ , taken by the camera are converted to film cooling effectiveness by Equation 2:

$$\eta = \frac{C_{\infty} - C_{mix}}{C_{\infty}} \quad (2)$$

In this equation  $C_{\infty}$  is the concentration of oxygen in the mainstream air flowing through the wind tunnel and  $C_{mix}$  is the concentration of oxygen at the plate surface as measured by the PSP. The result of this equation is a film cooling effectiveness value of 0 where there is no coolant such as upstream or far downstream of the holes, and a value of 1 inside the hole where the fluid is 100% coolant. This coolant mass fraction at the plate surface is directly correlated to the adiabatic wall temperature for the analogous heat transfer situation that occurs on a turbine blade surface.

In this experiment a 520 nm band pass filtered strobe is used to illuminate the particles. The light is driven by a function generator and is coupled with a 610 nm band pass filter camera that records images of the illuminated paint at approximately 3 Hz as shown in Figure 8. The intensity values are recorded as gray-scale TIFF images on the computer and are then converted to pressure data using a calibration curve. Images are recorded under four conditions for each test in order to obtain the film cooling effectiveness: a

black image with no light and no mainstream flow, a reference image with light but no mainstream flow, mainstream flow and air as coolant, mainstream flow and nitrogen as coolant. Using these four images the film cooling effectiveness can be determined: the black and reference image serve to remove noise, and the air image removes the static pressure effect so that only the oxygen concentration effect from the nitrogen coolant remains.

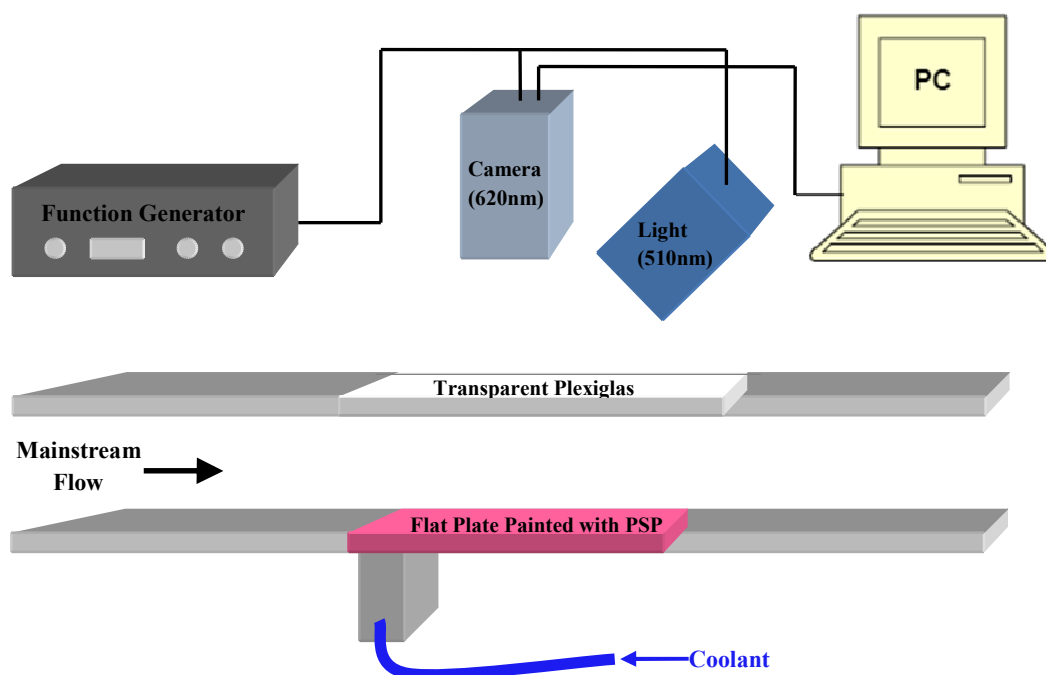


**Figure 8: Experimental setup for PSP data acquisition**

The PSP calibration is conducted by placing a painted sample in a vacuum as shown in Figure 9 and slowly releasing air into the chamber. At several discrete points between vacuum and atmosphere, intensity values are recorded by camera images and matched with the pressure indicated on a dial gauge. These values yield a calibration curve that can then be used to translate intensities to pressures. The calibration curve used for these experiments is shown in Figure 10.

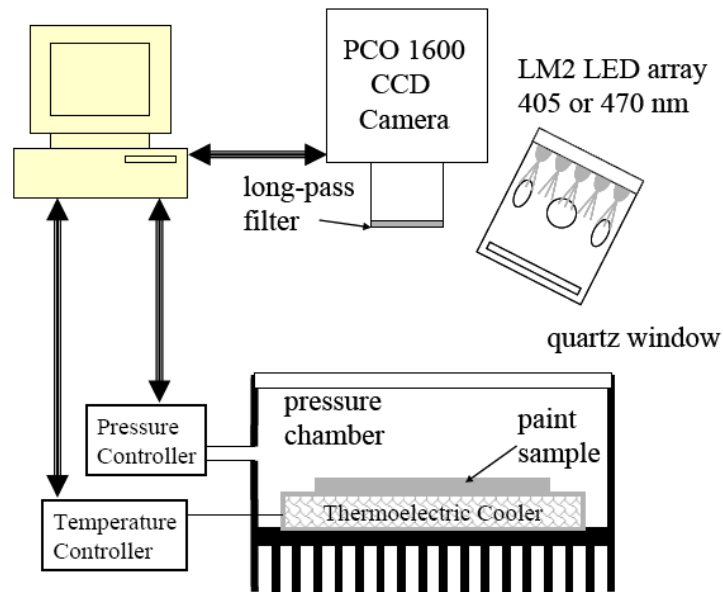


Figure 9: PSP calibration apparatus

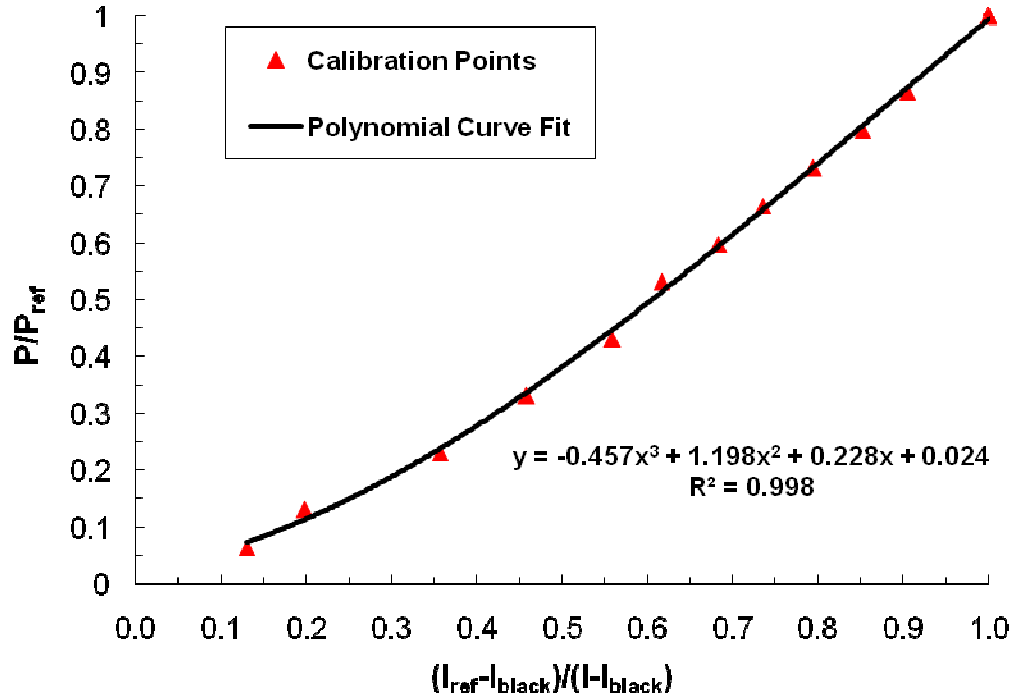


Figure 10: PSP calibration curve

## Procedure

The flow conditions tested to study density effect are shown in Table 1. The density ratio of 0.93 was achieved by using air at 50°C as the coolant while the mainstream air was at 23°C. To achieve the density ratio of 1.47, CO<sub>2</sub> at 50°C was used as the coolant under the same mainstream flow conditions. One advantage of using two different gases at the same temperature to study density effect is that the conduction effect is similar in each because of an identical temperature difference across the plate.

**Table 1: Test conditions for density ratio effect**

<b>Test No</b>	<b>Plate</b>	<b>Density Ratio</b>	<b>Blowing Ratios</b>
<b>1</b>	Cylindrical Simple Angle	0.93	0.3, 0.6, 1.0, 1.5
<b>2</b>	Cylindrical Simple Angle	1.47	0.3, 0.6, 1.0, 1.5
<b>3</b>	Cylindrical Compound Angle	0.93	0.3, 0.6, 1.0, 1.5
<b>4</b>	Cylindrical Compound Angle	1.47	0.3, 0.6, 1.0, 1.5

In the course of our testing we explored the conduction on the plate and how it affects the results over time. Through this process an experimental procedure was developed through which values for the film cooling effectiveness were recorded relatively free from conduction errors. This procedure involved taping the holes shut, purging coolant through the plenum to heat it, and running the wind tunnel at test condition; this allowed the coolant to reach 50°C in the plenum and the plate to reach a steady state for conduction from the plenum that can be isolated and removed from the results. The conduction through the plate from the plenum at steady state proved to be relatively insignificant but the conduction along the plate surface around the areas covered by the coolant jet was very significant. In order to isolate the film cooling effectiveness without conduction errors the tape covering the holes was removed by hand while at steady state flow and data was recorded immediately. Through experimentation with this method the conduction effect was investigated and isolated as explained in the results.

The upstream step effect was studied under the test conditions shown in Table 2. Using the PSP painted flat plate and the filtered camera for each of the conditions shown, images were recorded using room temperature air, and CO<sub>2</sub> as the coolant.

**Table 2: Test conditions for step effect**

<b>Test No</b>	<b>Plate</b>	<b>Step Height</b>	<b>Blowing Ratios</b>
<b>1</b>	Cylindrical Simple Angle	0 mm	0.3, 0.6, 1.0, 1.5
<b>2</b>	Cylindrical Simple Angle	0.5 mm	0.3, 0.6, 1.0, 1.5
<b>3</b>	Cylindrical Simple Angle	1 mm	0.3, 0.6, 1.0, 1.5
<b>4</b>	Cylindrical Simple Angle	1.5 mm	0.3, 0.6, 1.0, 1.5
<b>5</b>	Cylindrical Compound Angle	0 mm	0.3, 0.6, 1.0, 1.5
<b>6</b>	Cylindrical Compound Angle	0.5 mm	0.3, 0.6, 1.0, 1.5
<b>7</b>	Cylindrical Compound Angle	1 mm	0.3, 0.6, 1.0, 1.5
<b>8</b>	Cylindrical Compound Angle	1.5 mm	0.3, 0.6, 1.0, 1.5



## RESULTS

### **Conduction Effect**

Understanding the conduction effect on the flat plate was a prerequisite for the study of density effect using the IR method. As explained in the experimental procedure section, a method was developed by which images could be recorded immediately after the coolant began to flow through the holes into the mainstream. The results of this procedure produced Figure 11, which shows the spanwise average effectiveness at a series of times after the coolant flow began. This clearly shows the average effectiveness rising through 300 seconds, which is well after the flow is developed and can only be the result of conduction. This conduction is not the result of heat from the plenum though as suggested by previous studies; it is rather the effect of conduction along the plate surface outward from the area covered by the coolant jet.

Using the data displayed in Figure 12, the transition point when the increasing effectiveness is no longer due to flow development but is caused by conduction error can be identified. In this case the point occurred about 3 seconds after the coolant flow began, but for recording consistent relatively error free data, the image taken 4 seconds after the flow began was used for comparing the results of various test conditions.

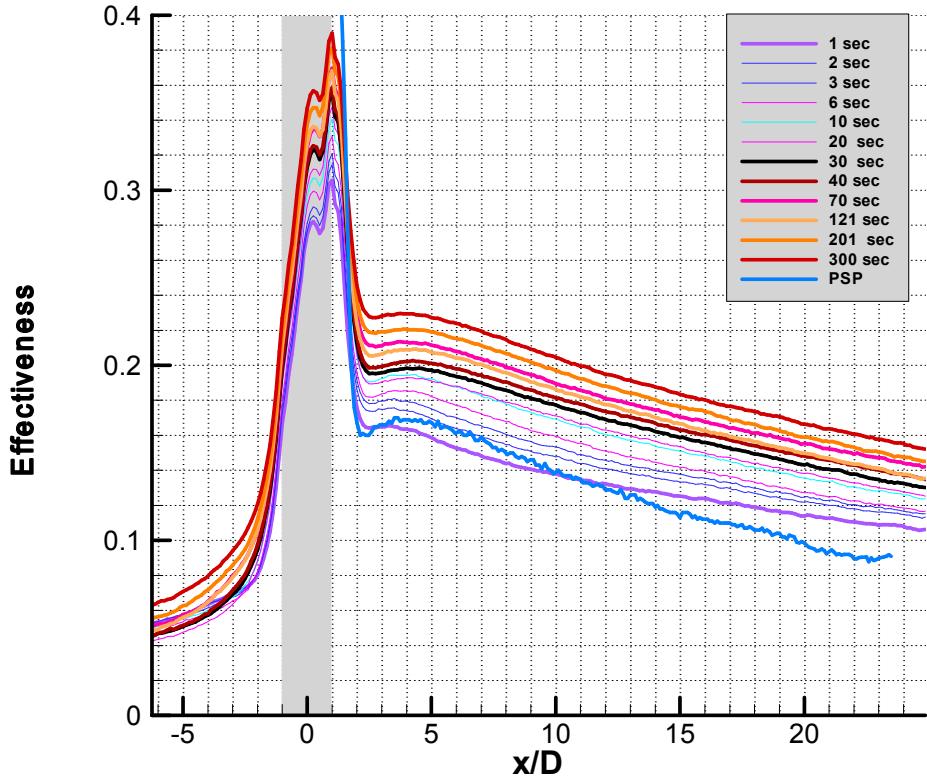


Figure 11: Conduction effect over 5 minutes

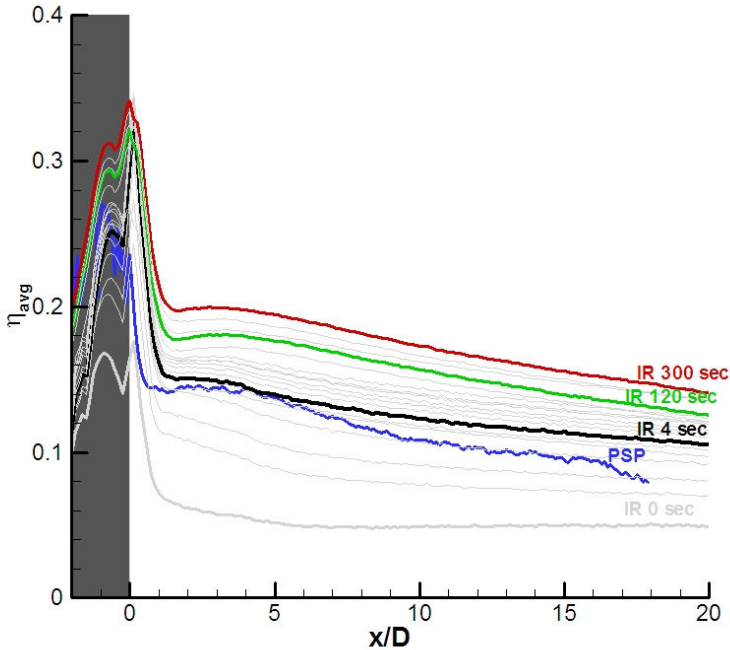


Figure 12: Conduction effect on spanwise averages over time

Figure 13 shows a comparison of the PSP data to previous studies. The current study falls in line with previous studies such as Goldstein et al. [4] and therefore provides validation of the PSP method used to seek conduction free IR data.

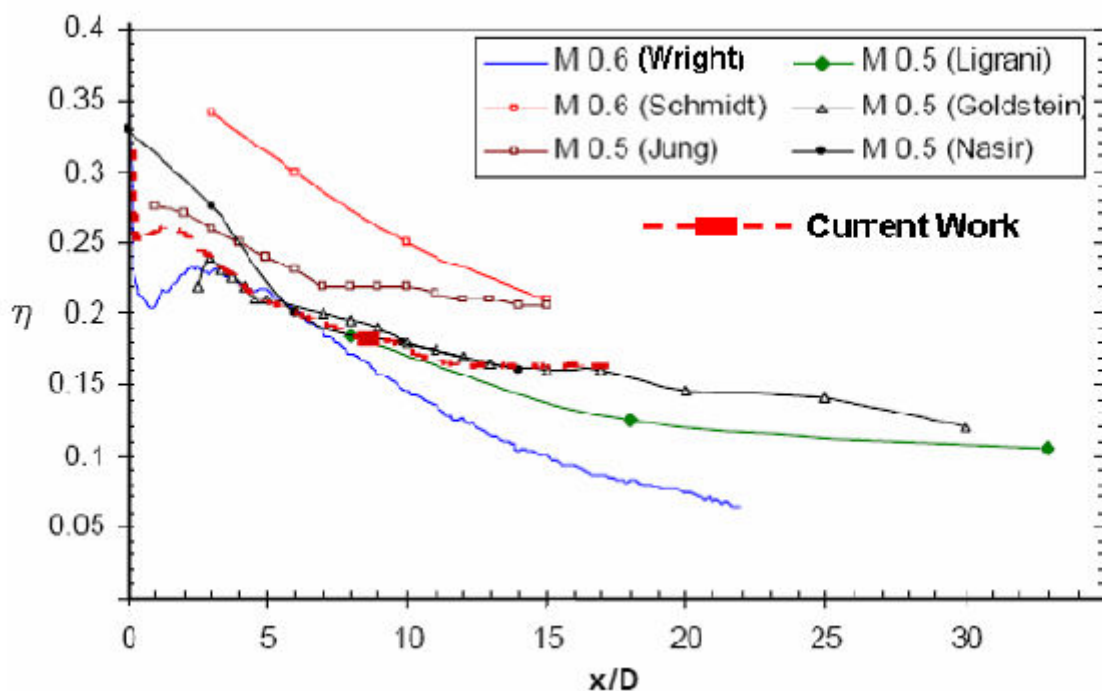


Figure 13: Comparison of current study to previous studies

### Density Effect

Figure 14 shows the density effect on the plate with cylindrical simple angle film cooling holes. These images are an average of two tests at the same condition to yield greater accuracy. The images on the left are at a coolant to mainstream density ratio of 0.97 and on the right 1.47. Shown are the images for all three blowing ratios 0.3, 0.6, 1.0 and 1.5. The images show the effectiveness to be greater at the higher density ratio, particularly near the holes. This is because the dense coolant is more inclined to flow along the plate surface and does not separate as quickly as the less dense coolant. This is the same trend seen in previous research but the results presented here are more precise, being free from conduction error, which can obscure the clarity of the conduction effect.

Additionally, the density effect is more pronounced at higher blowing ratios because the higher momentum of the coolant results in greater flow separation and lower film cooling effectiveness, which higher density coolant tends to reduce.

Figure 15 shows the density effect on the plate with cylindrical compound angle holes. The density effect is very similar to the simple angle holes except less pronounced because coolant flowing from the compound angle holes has less of a tendency to separate from the plate surface.

Figure 16 shows the spanwise average effectiveness of the 0.93 density ratio (air) and the 1.47 ( $\text{CO}_2$ ) for the simple angle holes at a blowing ratio of 0.6. This clearly shows the increased density ratio results in high film cooling effectiveness particularly near the holes.

Figure 17 shows the spanwise averages for the compound angle holes and again the higher density ratio results in higher film cooling effectiveness but not of the same magnitude as with the simple angle holes.

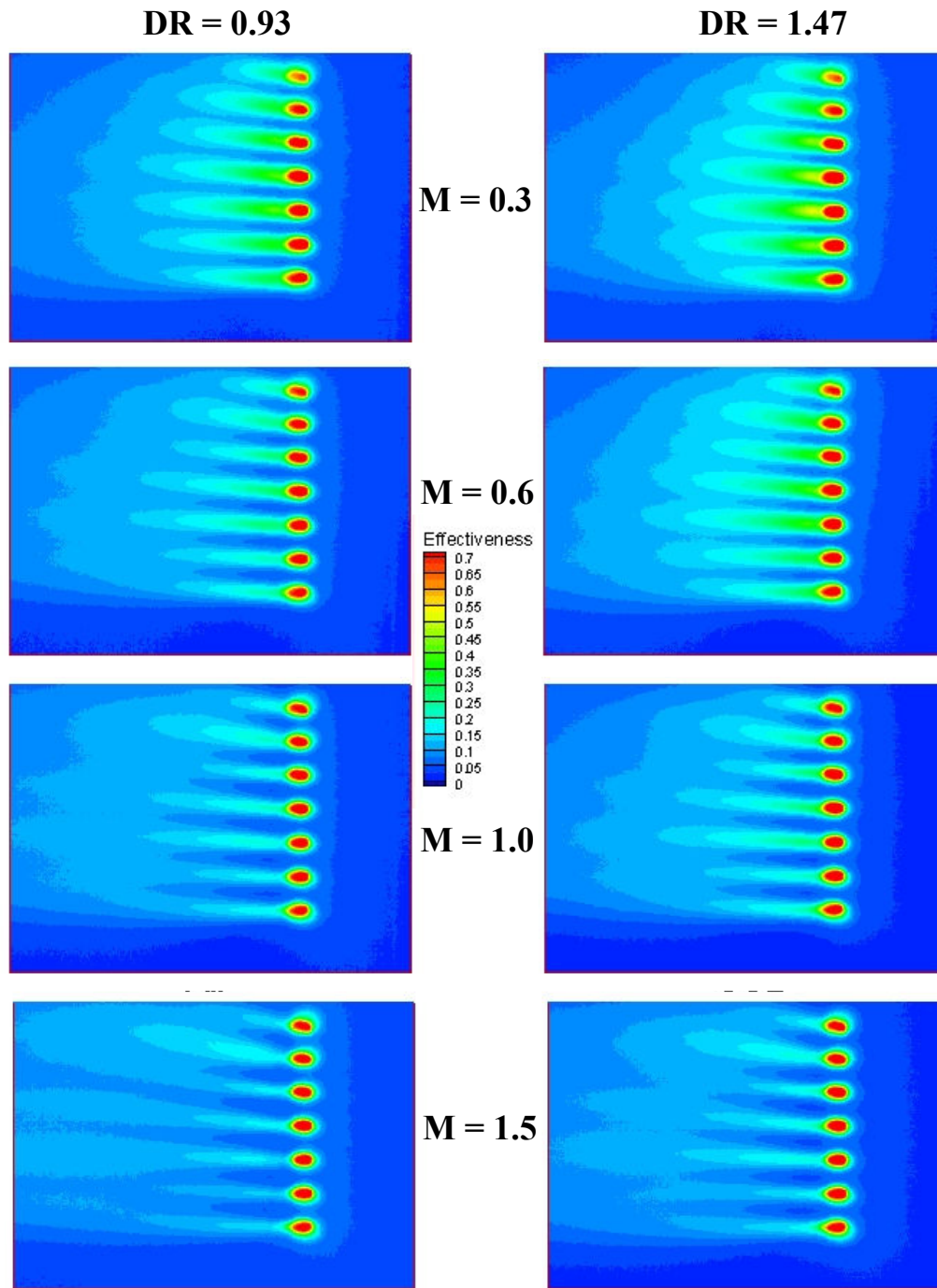


Figure 14: Contour plots of simple angle hole density effect at various blowing ratios

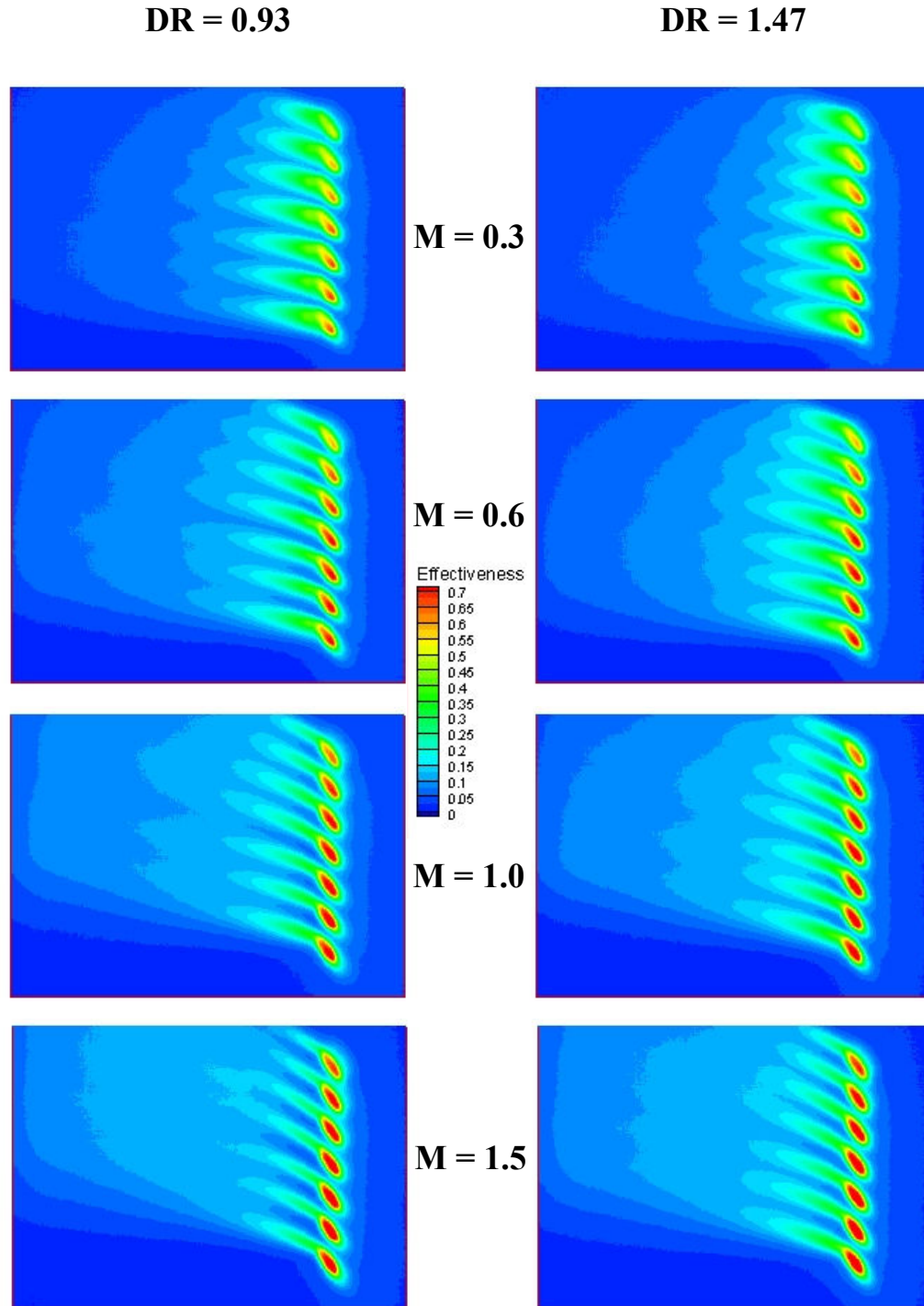


Figure 15: Contour plots of compound angle hole density effect at various blowing ratios

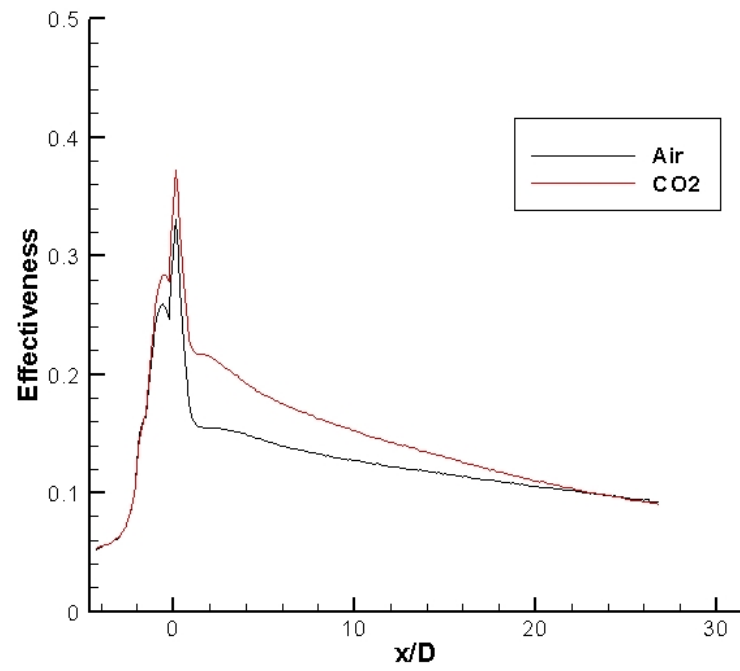


Figure 16: Spanwise average of effectiveness of simple angle holes at  $M=0.6$

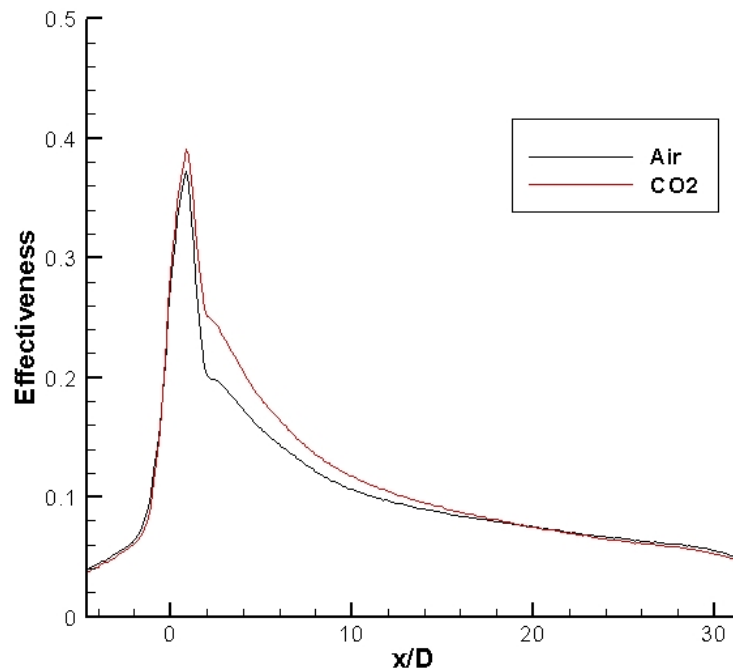


Figure 17: Spanwise average of effectiveness of compound angle holes at  $M=0.6$

### Upstream Step Effect

Figure 18 shows the contour plots of film cooling effectiveness on the flat plate with simple angle holes for four different blowing ratios, as recorded by the PSP method. These images were recorded with no upstream step and serve as a base case for comparing the results of adding an upstream step. Figures 19, 20, and 21 show the film cooling effectiveness for the simple angle plate with a 0.5, 1.0, and 1.5 mm upstream step respectively. The step was placed at the upstream edge of the holes and can be seen in the images to significantly raise the cooling effectiveness around and just downstream of the holes. Previous studies that tested the effect of a step 0.5-2 D upstream of the holes showed little or no effect on cylindrical holes. The results presented here indicate that the effect is significant around the holes and in some of the cases even downstream.



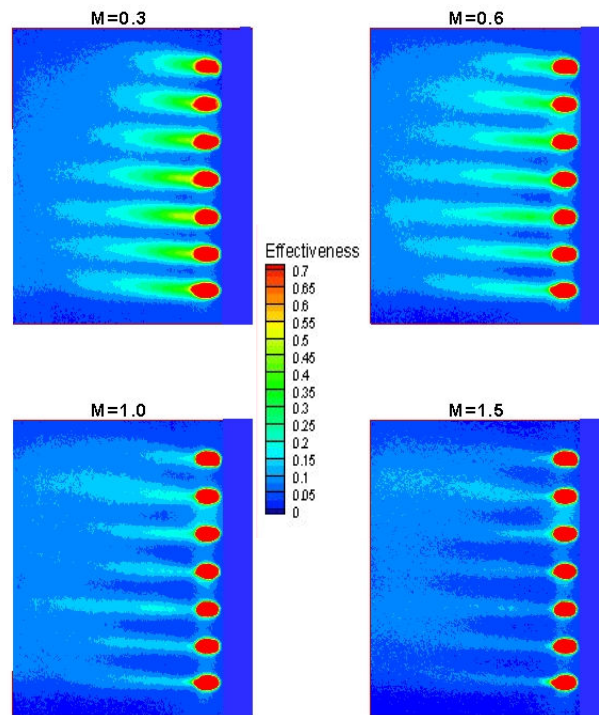


Figure 18: PSP film cooling effectiveness for cylindrical simple angle holes with no step

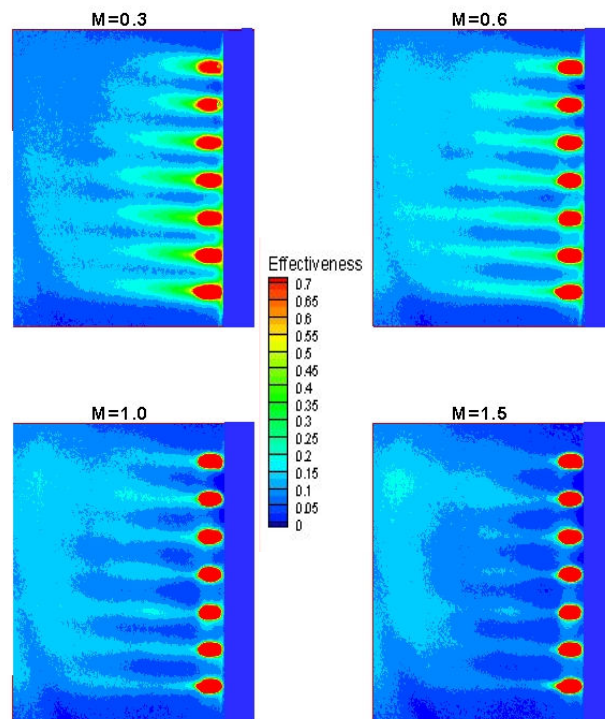


Figure 19: PSP film cooling effectiveness for cylindrical simple angle holes with 0.5 mm step

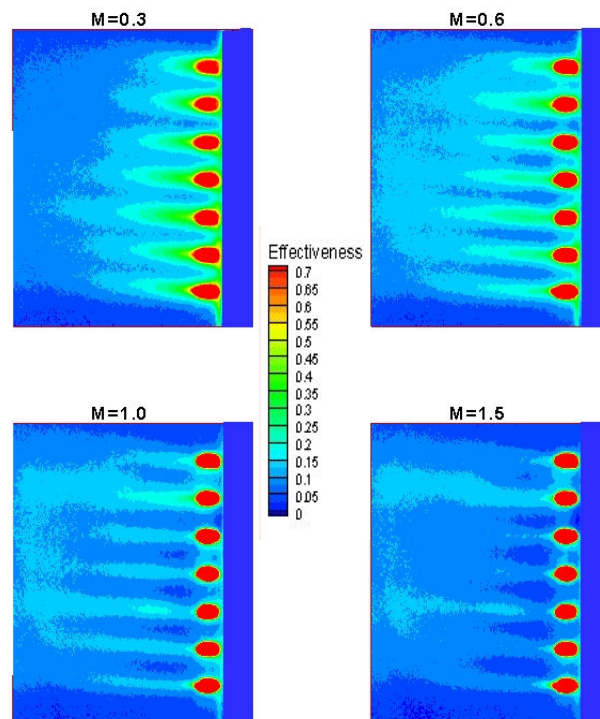


Figure 20: PSP film cooling effectiveness for cylindrical simple angle holes with 1 mm step

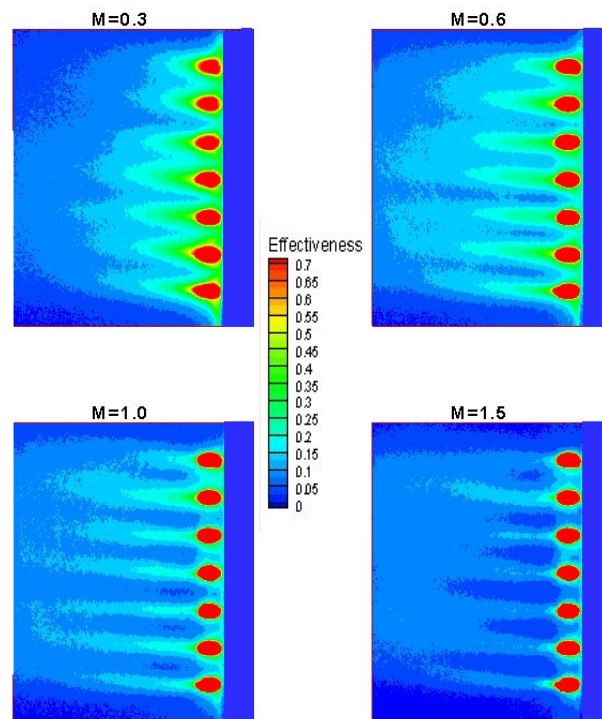


Figure 21: PSP film cooling effectiveness for cylindrical simple angle holes with 1.5 mm step

Figure 22 shows the spanwise effectiveness averages for the three step sizes and no step at  $M = 0.6$ . The graph shows slightly higher effectiveness with the 0.5 and 1 mm, and significantly higher effectiveness with 1.5 mm on the order of 10% near the holes. On a simple angle plate this represents a significant difference from previous studies which indicated that effectiveness was unaffected by a step only 0.5D upstream. Spanwise plots for the other blowing ratios are shown in the appendix.

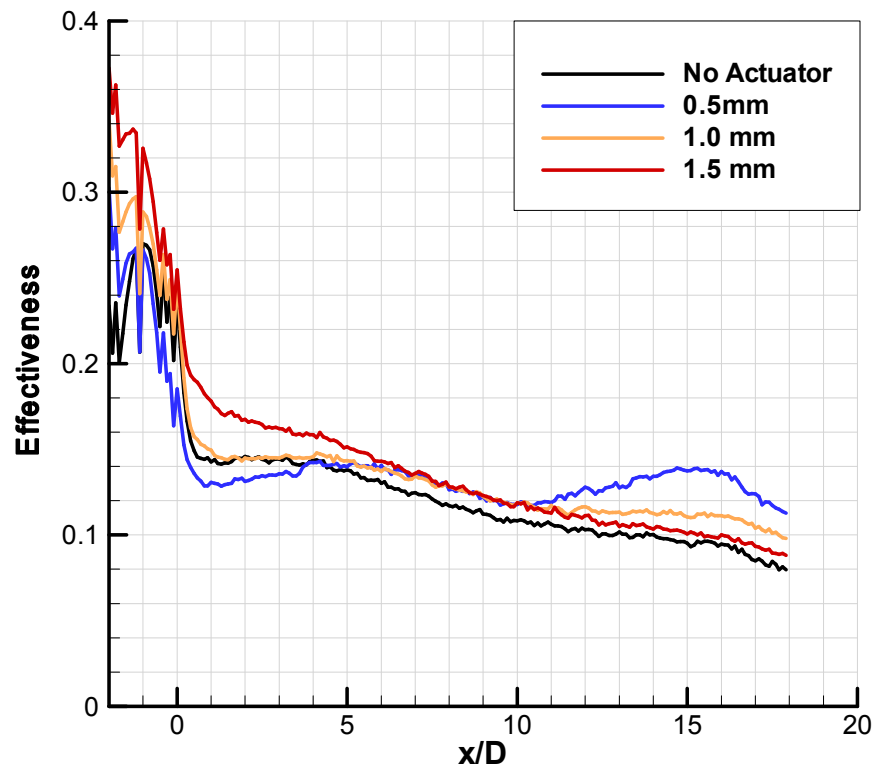
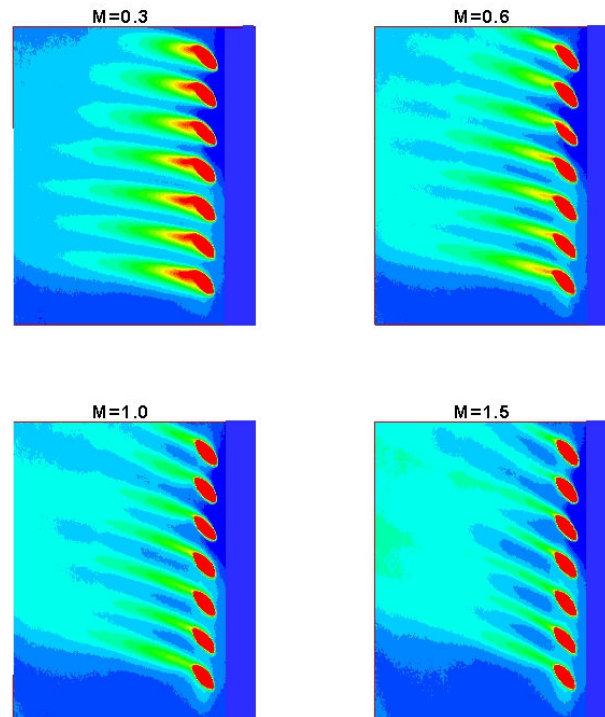


Figure 22: Spanwise effectiveness for various upstream steps on simple angle plate at  $M = 0.6$

Figure 23 shows the PSP recorded film cooling effectiveness for the plate with compound angle holes and no upstream step. As anticipated the compound angle holes result in higher effectiveness than simple angle holes at the same blowing ratio. Figures 24, 25 and 26 show the compound angle plate with 0.5, 1.0 and 1.5 mm steps placed directly upstream of the holes. The steps have a much greater impact on film cooling effectiveness on the compound angle plate than on the simple angle. This is consistent

with previous literature but again, the degree to which the step effect impacts the film cooling effectiveness is much greater in this test than in literature, likely due to the placement of the step directly at the upstream edge of the holes. Figure 27 shows the effectiveness spanwise averages for the compound angle plate with the various steps at a blowing ratio of  $M = 0.6$ . The figure shows a consistent trend of increased effectiveness as the step size increases and with the 1.5 mm step the effectiveness near the holes is increased as much as 60%. Spanwise plots for the additional blowing ratios are shown in Appendix B.



**Figure 23: PSP film cooling effectiveness for cylindrical compound angle holes with no step**

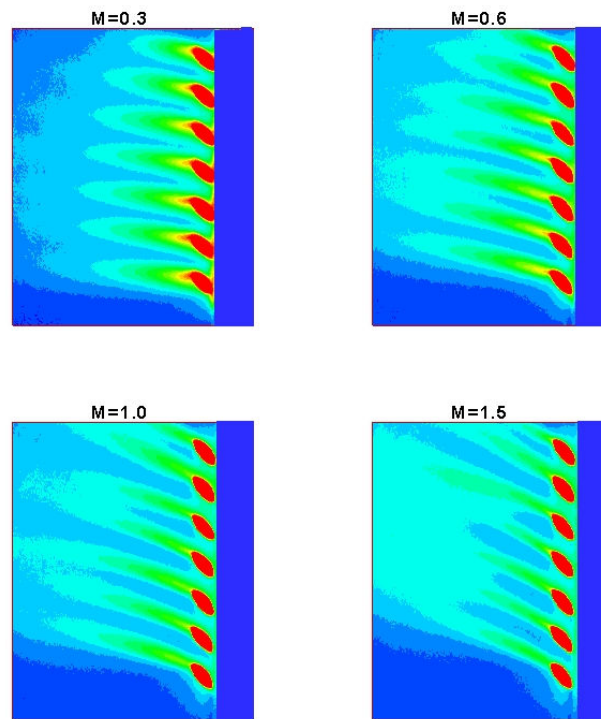


Figure 24: PSP film cooling effectiveness for cylindrical compound angle holes with 0.5 mm step

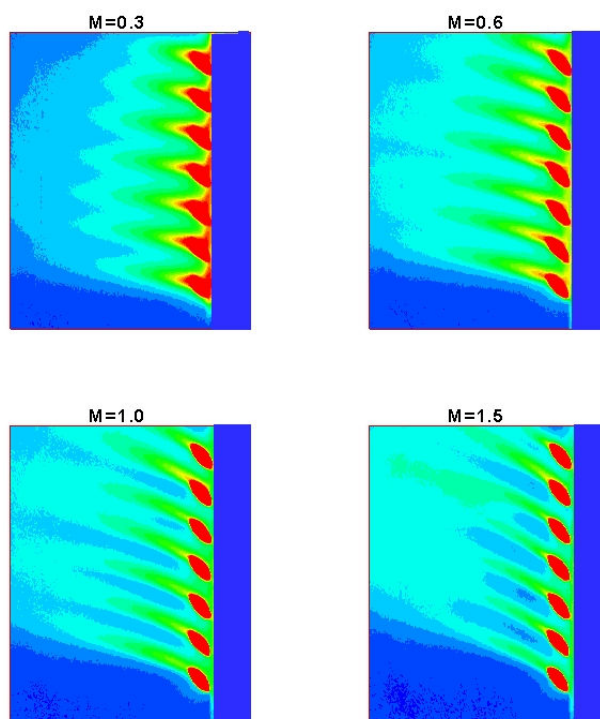


Figure 25: PSP film cooling effectiveness for cylindrical compound angle holes with 1.0 mm step



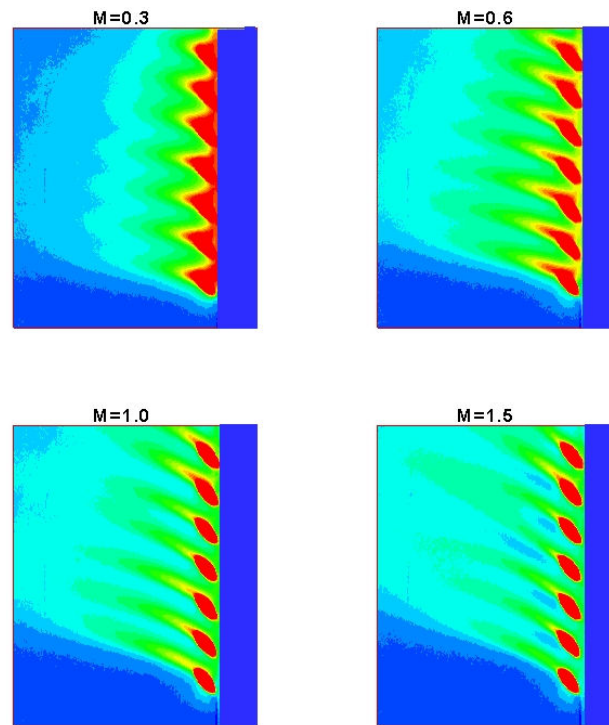


Figure 26: PSP film cooling effectiveness for cylindrical compound angle holes with 1.5 mm step

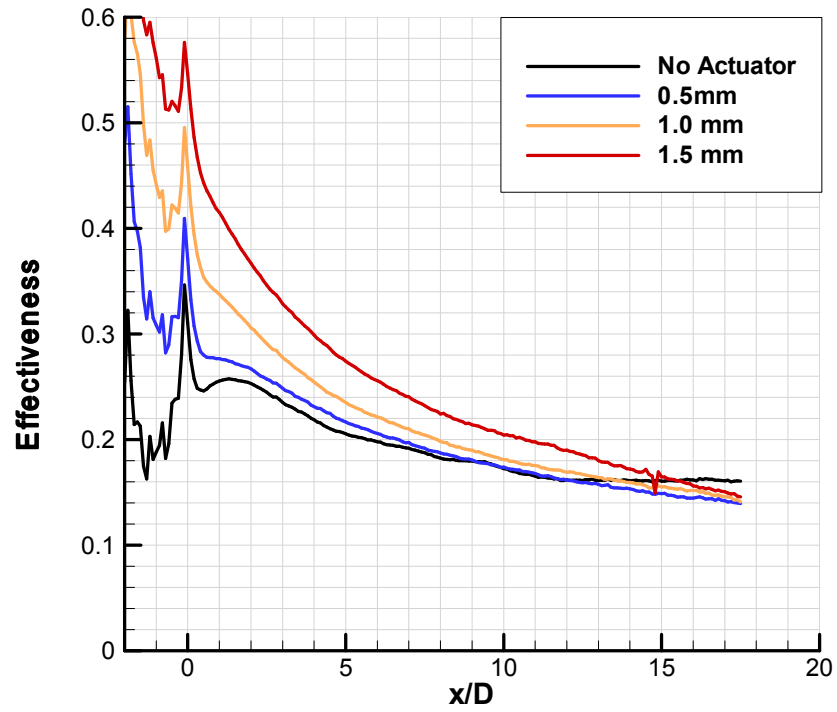


Figure 27: Spanwise effectiveness for various upstream steps on compound angle plate at  $M = 0.6$

## CONCLUSIONS

This experimental study focused on film cooling effectiveness on a flat plate in a low-speed wind tunnel; simulating film cooling holes on the blade of a turbine. Specifically, the effect of coolant to mainstream density ratio and the effect of an upstream step were studied at various coolant flow rates and at with two different cooling hole configurations. The objective of these experiments was to put further definition around these two effects.

During the study of density effect, more definition was put around the conduction error, one of the more challenging aspects of the thermographic IR measurement technique. The conduction was discovered to be much more prevalent along the surface of the flat plate than through the flat plate from the plenum as previously thought. Through this experiment, clear definition was put around the nature of the conduction error and a testing method was developed to eliminate it from the results. This represents a significant improvement in the methodology of thermography. Results recorded using this method showed similar trends as previous studies: higher density ratio resulting in higher effectiveness, particularly in the upstream portion of the plate; but the degree of the density effect was shown to be less than previously thought. Density effect trends among the different plates were also consistent with literature: higher effect on simple angle holes than on compound angle holes. The density effect study presented here is not comprehensive though, and it would be beneficial to continue further study of the effect using the new conduction error reducing test procedure.

The upstream step effect study revealed very interesting results when the step was placed at the upstream edge of the holes rather than  $0.5D$  or more upstream. The step resulted in slightly higher effectiveness around the holes in the simple angle case, and as much as a 60% increase in the compound angle case. Both of these results are a substantial departure from previous studies and show the tremendous importance of step placement. This could be a very significant factor in determining thermal barrier coating

applications which often result in a step near the holes. Additional studies could further define the parametric effect and whether the observations of this study hold true with other holes shapes.

## REFERENCES

- [1] Bunker, R., 2004, "A Review of Shaped Hole Turbine Film-Cooling Technology," ASME Journal of Heat Transfer, **127**, pp. 441-453.
- [2] Langston, L.S., "Secondary Flows in Axial Turbines – A Review," Annals of the New York Academy of Sciences, **934**, pp. 11-26.
- [3] Bogard, D. G., and Thole, K. A., 2006, "Gas Turbine Film Cooling," Journal of Propulsion and Power, **22**, pp. 249-270.
- [4] Goldstein, R.J., Eckert, E.G., and Burggraf, R., 1974, "Effects of Hole Geometry and Density on Three Dimensional Film-cooling," International Journal of Heat and Mass Transfer, **17**, pp. 595–606.
- [5] Goldstein, R.J., Eckert, E.G., Eriksen, V.L., and Ramsey, J.W., 1970, "Film-cooling Following Injection Through Inclined Circular Tubes," Israel Journal of Technology, **8**, pp. 145-154.
- [6] Jubran, B., and Brown, A., 1985, "Film-cooling From Two Rows of Holes Inclined in the Streamwise and Spanwise Directions," ASME Journal of Engineering Gas Turbines Power, **107**, pp. 84–91.
- [7] Wright, L. M., Gao, Z., Varvel, T. A., and Han, J. C., 2005, "Assessment of Steady State PSP, TSP, and IR Measurement Techniques for Flat Plate Film Cooling," ASME paper no. HT2005-72363.

- [8] Bell, C. M., Hamakawa, H., and Ligrani, P. M., 2000, "Film Cooling From Shaped Holes," *ASME Journal of Heat Transfer*, **122**, pp. 224-32.
- [9] Sinha, A. K., Bogard, D. G., and Crawford, M. E., 1991, "Film-cooling Effectiveness Downstream of a Single Row of Holes with Variable Density Ratio," *ASME Journal of Turbomachinery*, **113**, pp. 442-9.
- [10] Pietrzyk, J. R., Bogard, D. G., and Crawford, M. E., 1989, "Effects of Density Ratio on the Hydrodynamics of Film Cooling," *ASME, Gas Turbine and Aeroengine Congress and Exposition*, pp. 8.
- [11] Jessen, W., Schroder, W., and Klaas, M., 2007, "Evolution of Jets Effusing from Inclined Holes into Crossflow," *International Journal of Heat and Fluid Flow*, **28**, pp. 1312-26.
- [12] Schmidt, D. L., Sen, B., and Bogard, D. G., 1994, "Film Cooling with Compound Angle Holes: Adiabatic Effectiveness," *ASME International Gas Turbine and Aeroengine Congress*, pp. 1-8.
- [13] Cutbirth, M. J., and Bogard, D. G., 2003, "Effects of coolant density ratio on film cooling performance on a vane," *ASME IGTI*, pp. 385-394.
- [14] Wayne, S. K., and Bogard, D. G., 2007, "High-resolution Film Cooling Effectiveness Measurements of Axial Holes Embedded in a Transverse Trench with Various Trench Configurations," *ASME Journal of Turbomachinery*, **129**, pp. 294-302.
- [15] Lu, Y., Dhungel, A., Ekkad, S. V., and Bunker, R. S., 2007, "Effect of Trench Width and Depth on Film Cooling from Cylindrical Holes Embedded in Trenches," *ASME Turbo Expo*, pp. 339-49.

- [16] Bunker, R. S., 2002, "Film Cooling Effectiveness Due to Discrete Holes Within a Transverse Surface Slot," ASME IGTI, **3**, pp. 129-38.
- [17] Harrison, K. L., Dorrington, J. R., Dees, J. E., and Bogard, D. G., 2007, "Turbine Airfoil Net Heat Flux Reduction with Cylindrical Holes Embedded in a Transverse Trench," ASME Turbo Expo, pp. 771-80.
- [18] Harrison, K. L., and Bogard, D. G., 2007, "CFD Predictions of Film Cooling Adiabatic Effectiveness for Cylindrical Holes Embedded in Narrow and Wide Transverse Trenches," ASME Turbo Expo, pp. 811-20.
- [19] Barigozzi, G., Franchini, G., Perdichizzi, A., 2007, "The Effect of an Upstream Ramp on Cylindrical and Fan-Shaped Hole Film Cooling – Part II: Adiabatic Effectiveness Results," ASME Turbo Expo, paper no. GT2007-27079.
- [20] Barigozzi, G., Franchini, G., Perdichizzi, A., 2007, "The Effect of an Upstream Ramp on Cylindrical and Fan-Shaped Hole Film Cooling – Part I: Aerodynamic Results," ASME Turbo Expo, paper no. GT2007-27077.
- [21] Young, C.D., Han, J.C., Huang, Y., and Rivir, R.B., 1992, "Influence of Jet-Grid Turbulence on Flat Plate Turbulent Boundary Layer Flow and Heat Transfer," ASME Journal of Heat Transfer, **114**, pp. 65-72.
- [22] Han, J.C., Dutta, S., and Ekkad, S.V., 2000, *Gas Turbine Heat Transfer and Cooling Technology*, Taylor and Francis, New York.

- [23] Dittmar, J., Schulz, A., and Wittig, S., 2003, "Assessment of Various Film Cooling Configurations Including Shaped and Compound Angle Holes Based on Large-Scale Experiments," *ASME Journal of Turbomachinery*, **125**, pp. 57-64.
- [24] Zhang, L.J. and Fox, M., 1999, "Flat Plate Film Cooling Measurements using PSP Gas Chromatograph Techniques," *Proc. Fifth ASME/JSME Joint Thermal Engineering Conference*, San Diego, CA.
- [25] Crafton, J., Lachendro, N., Guille, M, Sullivan, J.P., and Jordan, J.D., 1999, "Application of Temperature and Pressure Sensitive Paint to an Obliquely Impinging Jet," *AIAA Paper No. AIAA-99-0387*.
- [26] Liu, T., Campbell, B.T., Burns, S.P., and Sullivan, J.P., 1997, "Temperature- and Pressure- Sensitive Luminescent Paints in Aerodynamics," *Applied Mechanics Review*, **50**, No. 4, pp. 227 – 246.



**APPENDIX A**  
**SPANWISE AVERAGES FOR ALL DENSITY EFFECT FLOW CONDITIONS**

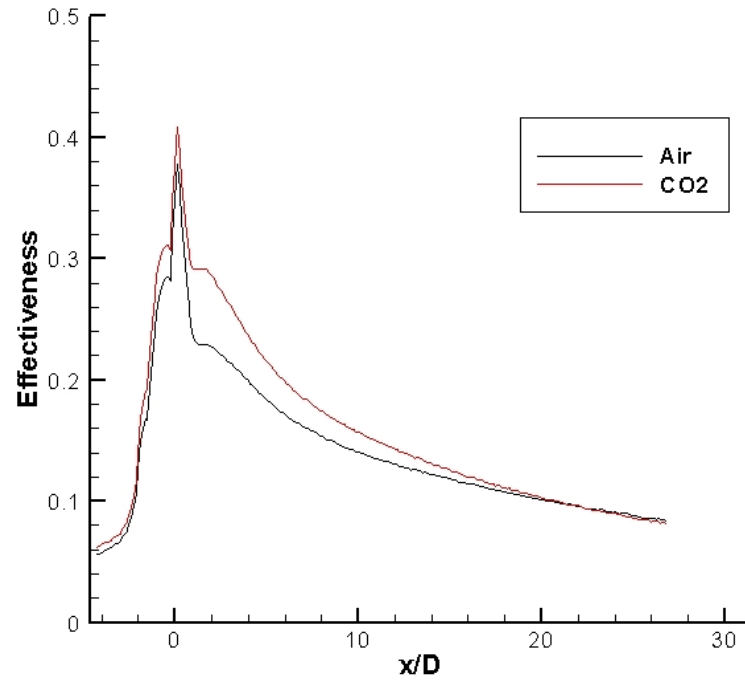


**Figure 28: PSP spanwise average of effectiveness of simple angle holes at M=0.3**

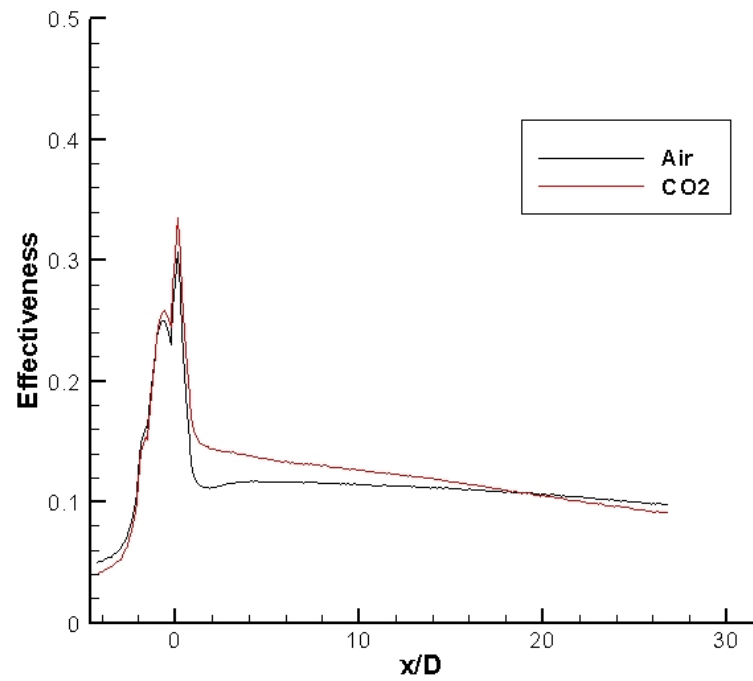


Figure 29: PSP spanwise average of effectiveness of simple angle holes at M=1.0

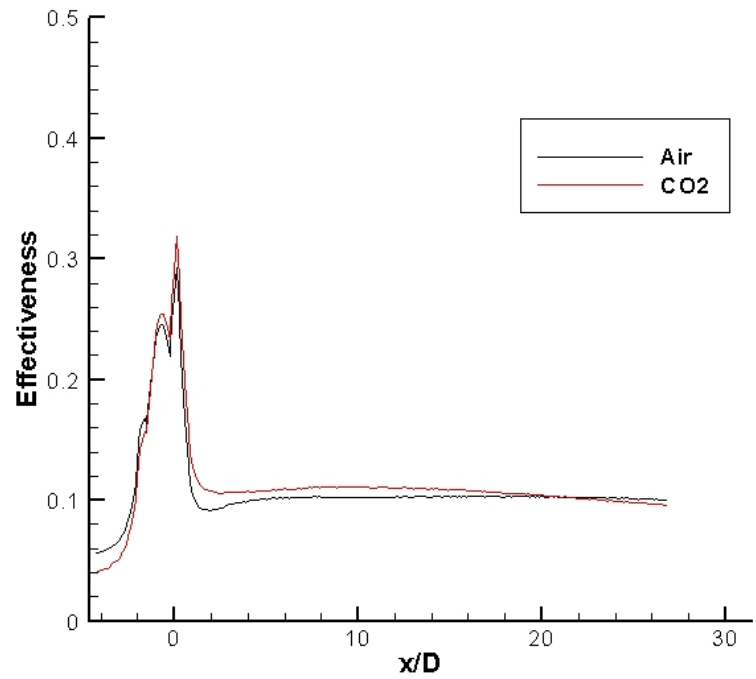


Figure 30: PSP spanwise average of effectiveness of simple angle holes at M=1.5

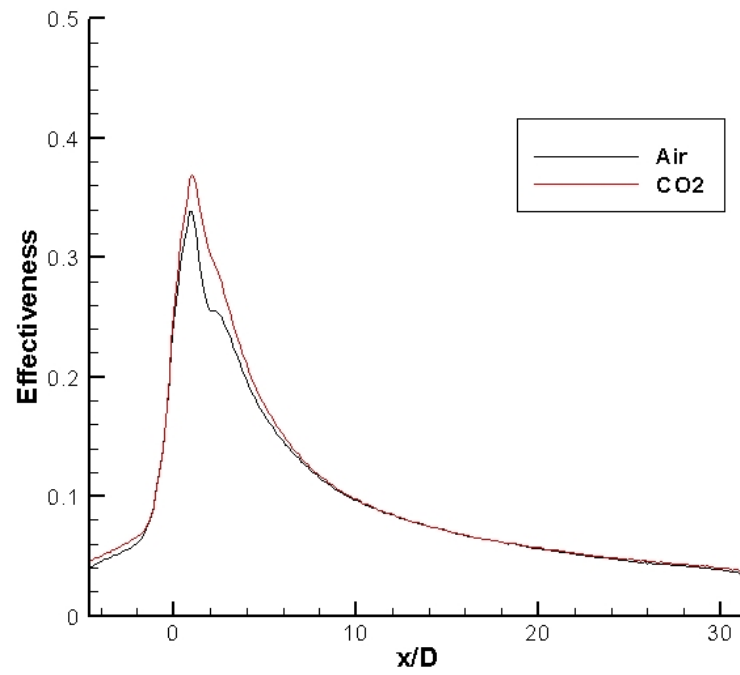


Figure 31: PSP spanwise average of effectiveness of compound angle holes at M=0.3

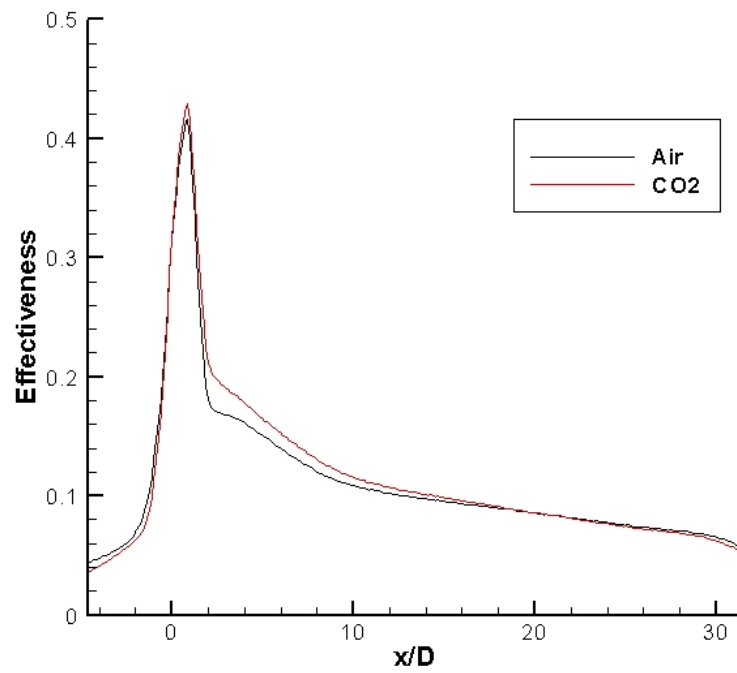


Figure 32: PSP spanwise average of effectiveness of compound angle holes at M=1.0

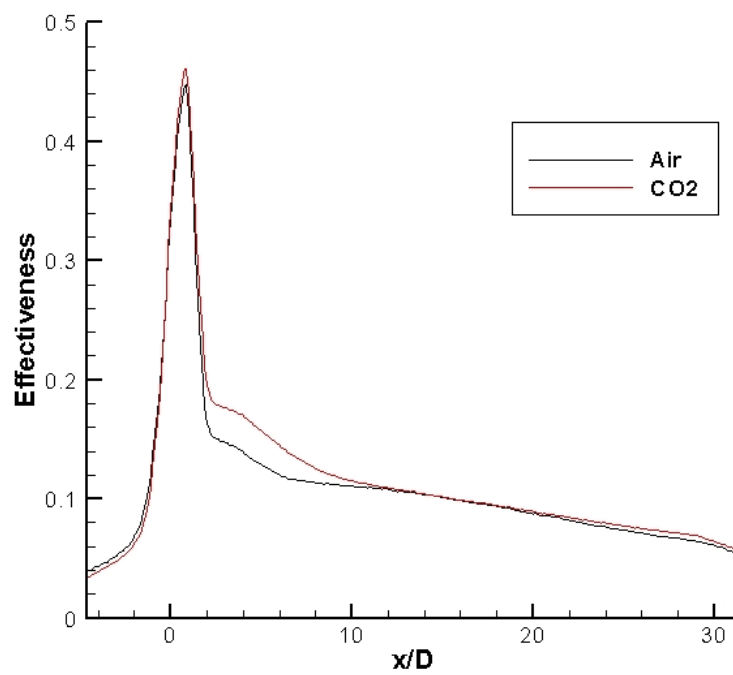


Figure 33: PSP spanwise average of effectiveness of compound angle holes at M=1.5

**APPENDIX B**  
**DETAILED STEP EFFECT RESULTS**

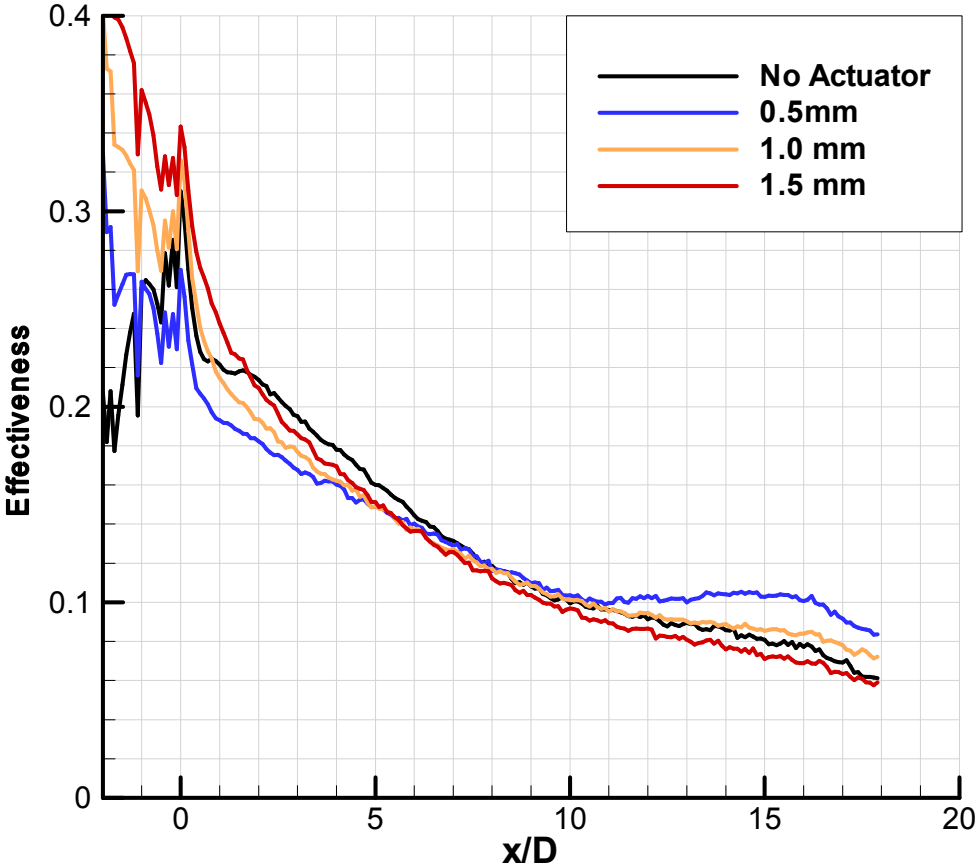


Figure 34: Spanwise effectiveness for various upstream steps on simple angle plate at M = 0.3

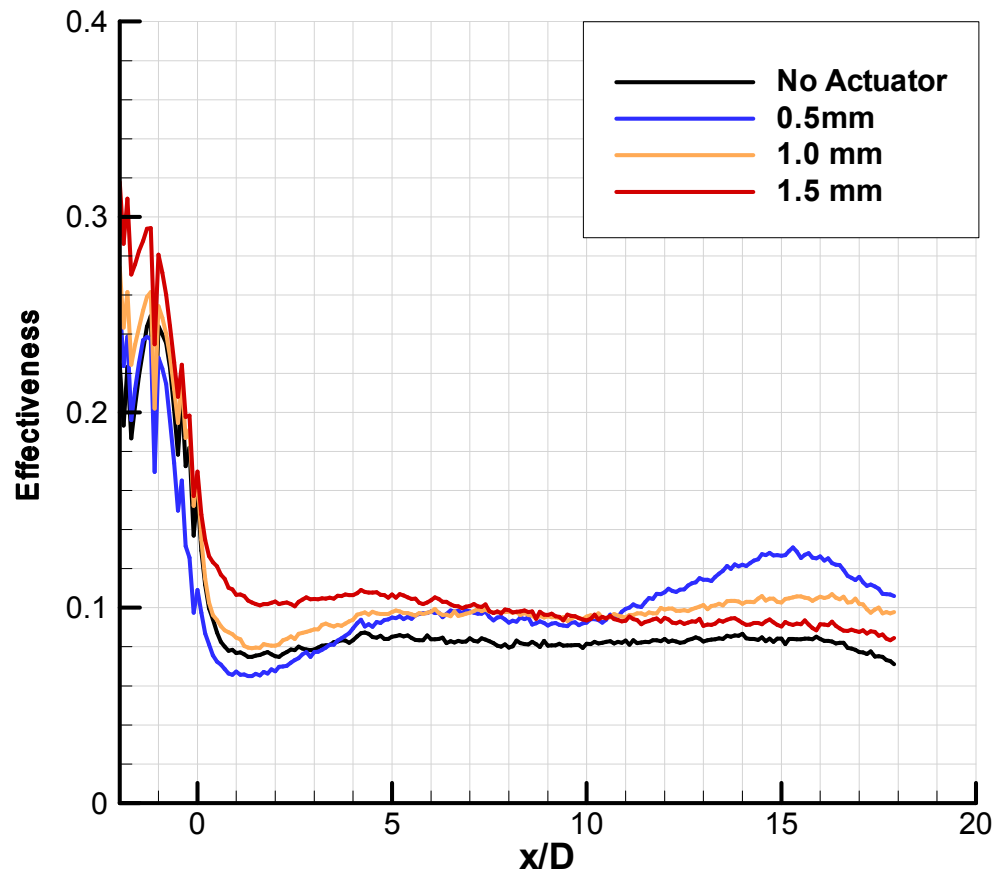


Figure 35: Spanwise effectiveness for various upstream steps on simple angle plate at  $M = 1.0$

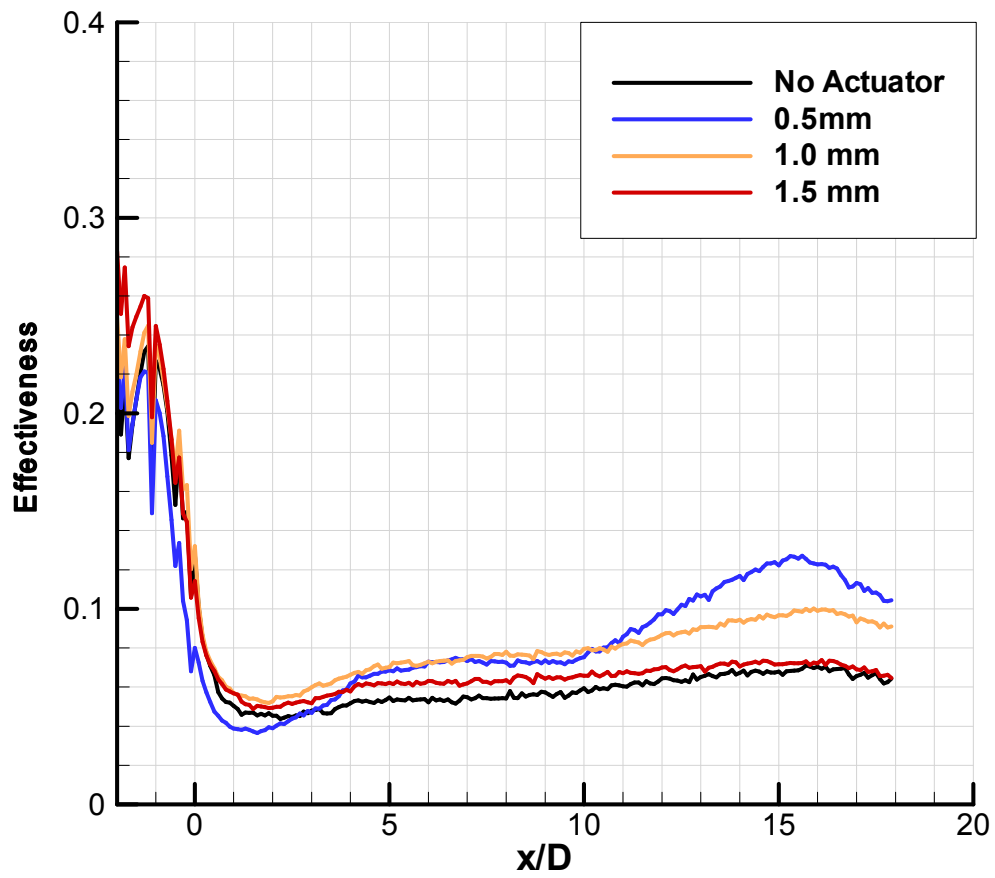


Figure 36: Spanwise effectiveness for various upstream steps on simple angle plate at  $M = 1.5$

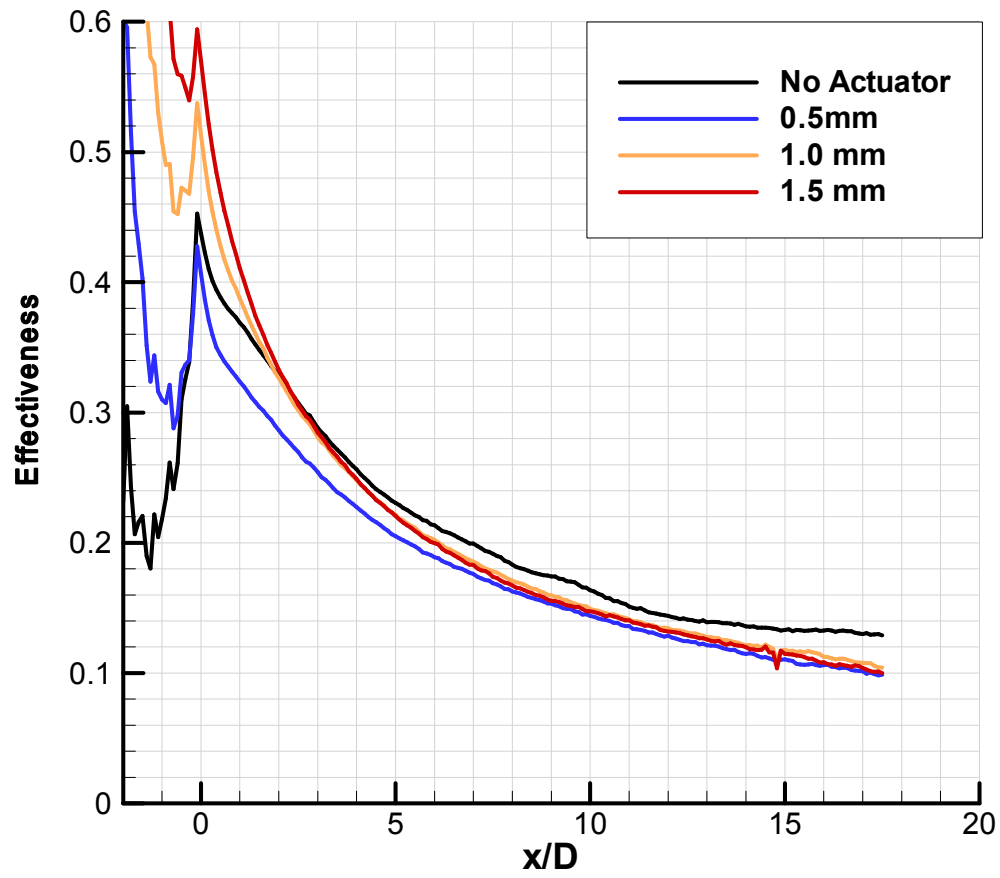


Figure 37: Spanwise effectiveness for various upstream steps on compound angle plate at  $M = 0.3$



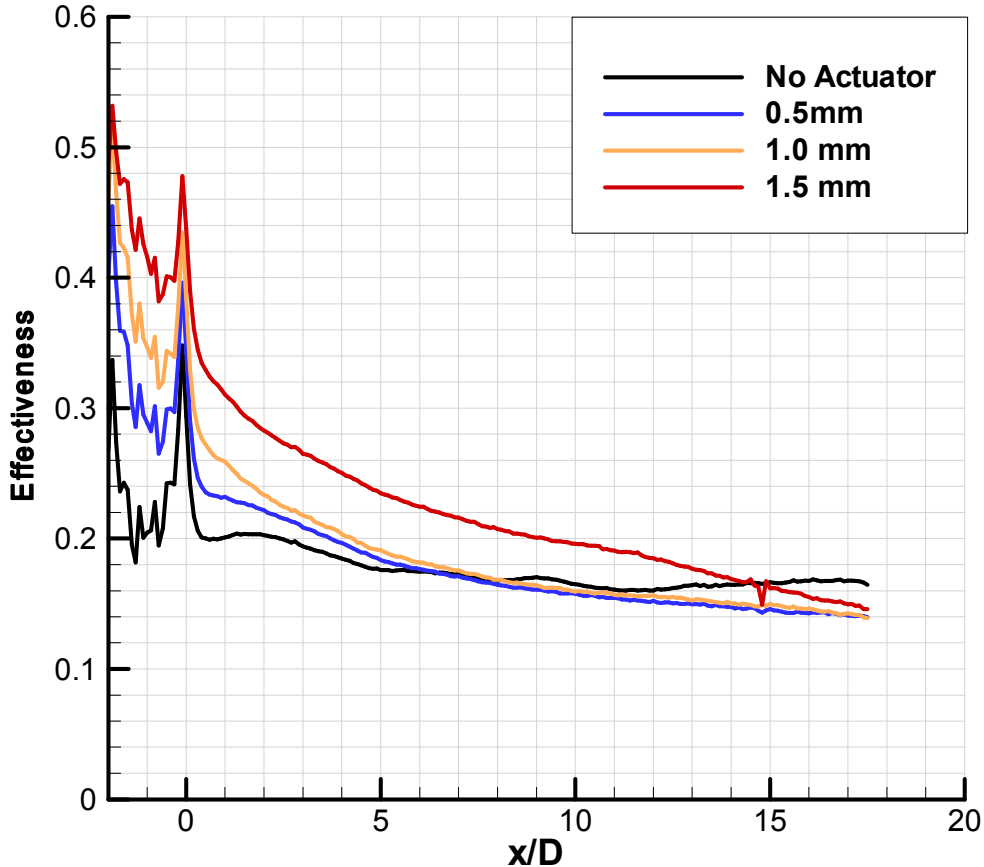


Figure 38: Spanwise effectiveness for various upstream steps on compound angle plate at M = 1.0

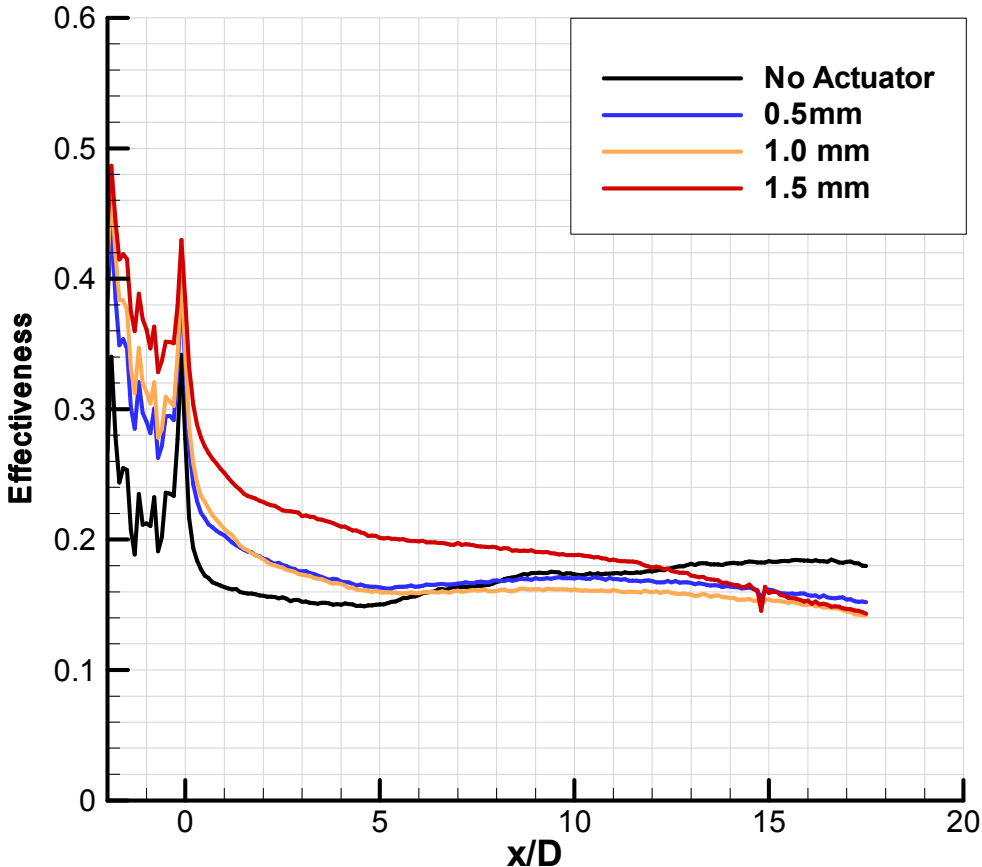


Figure 39: Spanwise effectiveness for various upstream steps on compound angle plate at M = 1.5

**VITA**

Name: Joshua P. F. Grizzle

Mailing Address: Turbine Heat Transfer Laboratory  
Texas A&M University  
3123 TAMU  
College Station, TX 77843

Email Address: [joshua.grizzle@gmail.com](mailto:joshua.grizzle@gmail.com)

Hometown: New York, NY

Education: Bachelor of Science, 2007  
Mechanical Engineering  
Texas A&M University  
College Station, Texas

Master of Science, 2008  
Mechanical Engineering  
Texas A&M University  
College Station, Texas